地理科学学院博士研究生贾恪2024年博士学位论文答辩及科研成果公示

2024年5月地理科学学院理学专业博士研究生贾恪完成博士学位论文答辩，答辩委员会一致同意该研究生通过博士学位论文答辩，建议授予理学博士学位。该生在读期间发表论文及佐证材料公示如下：

学号	姓名	专业	论文名称	刊物名称	发表情况	期刊类别	发表时间	是否达到学术论文发表要求
20196019002	贾恪	地理学	Temporary and spatial variation of vegetation in Net Primary Productivity of the Shendong Coal Mining area Inner Mongolia Autonomous Region	Sustainability	见刊	SCI	2022	是
20196019002	贾恪	地理学	NPP spatio-temporal change characteristics and contribution analysis of land-use type in the Shengdong Minigng area	Arabian journal of geosciences	见刊	SCI	2023	是

地理科学学院

2024年5月31日

sustainability

MDPI

.Article

Temporal and spatial variation of vegetation in net primary productivity of the Shendong coal mining area, Inner Mongolia Autonomous Region

Jia Ke[1,2], Dandan Zhou[1*], Chunxing Hai[1*], Yanhua Yu[2], Hao Jun[2], Bingzi Li[2]

College of Geographical Science, Inner Mongolia Normal University,Hohhot 010022,China;2.Inner Mongolia Institute of Territorial Space Planning,Hohhot 010018,China

Abstract: Coal mining can cause significant local environmental damage while driving the regional economy of an area. The key index of net primary productivity (NPP) measures the amount of energy made available in an ecosystem and serves as a useful metric for understanding vegetation restoration in mining areas. This study used a CASA model to estimate the vegetation NPP of the Ordos area of the Shendong coal fields from 2000 to 2019. Model output, human factors, and regional meteorological data were subjected to trend analysis, significance testing, partial correlation analysis, and residual analysis. The NPP data generated by a CASA model inversion approximated measured data to a reasonable degree. The average annual NPP of the vegetation in the study area from 2000 to 2019 was 44.51 g C /m^2 a. In general, NPP showed a fluctuating upward trend with slower increases before 2011 and more rapid increases after 2011. The trend exhibited considerable spatial heterogeneity. Areas with increasing NPP accounted for 21.54% of the study area and occurred mainly in Dongsheng District, Kangbashi District, and areas bordering Ijinhoro Banner. Analysis detected consistent spatial variation between NPP and each factor in the study area. NPP is positively correlated with precipitation and human activities, and negatively correlated with air temperature. The change in vegetation cover depended on both human activity and meteorological conditions. In terms of the strength of influence on vegetation NPP, human activity exceeded climate, followed by temperature and precipitation. Although the NPP of vegetation in the region directly affected by coal mining shows a trend of improvement, it is still lower than that in the natural growing region. In the next step, the ecological restoration of vegetation should be further strengthened to achieve regional ecological balance.

Keywords: net primary productivity (NPP); CASA; Shendong Mine; impact factor

Citation: Ke, J.; Zhou, D.; Li, B. Temporal and spatial variation in net primary productivity of the Shendong coal mining area, Inner Mongolia Autonomous Region. *Sustainability* **2022**, *14*, x. https://doi.org/10.3390/xxxxx

Academic Editor(s):

Received: date
Accepted: date
Published: date

1. Introduction

Modern civilization depends strongly on hydrocarbon-based energy sources (Fang et al., 2018), which have generally progressed from wood to whale oil, to coal, to oil and gas. Coal has driven industrialization, electrification, and transportation to support the expansion of human survival and material culture (Jiang et al., 2008). Countries experiencing rapid economic development based on coal energy sources find their economic base and stability to be tied to coal production (Yao et al., 2012). The Inner

Corresponding author: Chunxing Hai (1963-),male,professor.E-mail :hcxjs@imnu.edu.cn

Co-corresponding author: Dandan Zhou(1982-),female, Associate professor .E-mail:zhoudandan@imnu.edu.cn

Foundation item: Technology of site quality improvement in mining subsidence area(Inner Mongolia Autonomous Region key research and development project.Number: ZDZX2018058)

The author: Jia Ke (1987-), male, Ph.D student.E-mail :1303236349@qq.com

Mongolia Autonomous Region is a key area of China's westward migrating coal mining strategy (Xiao et al., 2019). Its coal resources are widely but densely distributed in the Mengdong and Mengzhong mining areas (Wang et al., 2012). Together, these represent a hundred million tons of the national large coal base. The Mengzhong mining area is located in Ordos City, Inner Mongolia and includes the Shendong coal fields. The area hosts thick, undeformed coal seams suitable for large-scale, mechanized subsurface mining. The area overlying the mines represents an ecologically fragile area subject to subsidence and collapse. In the case of subsidence and collapse, mining of subsurface coal seams removes support and thereby disrupts the overlying surface. Mine subsidence has harmed vegetation, soil, and other aspects of the local ecosystem. Negative environmental detract from the economic benefits of large-scale mining (Li et al., 2009). Over time, the original ecological vegetation is gradually degraded and only distributed in sporadic areas. Relatively speaking, the proportion of artificial vegetation increases year by year (Li et al., 2011). Vegetation represents a major component of terrestrial ecosystems and a key factor for measuring their health (Ge et al., 2021). Net vegetation primary productivity (vegetation NPP) tracks energy flows and overall ecosystem health. NPP also measures an area's contribution to the global carbon cycle.

To date, the primary methods for estimating NPP have been field measurements or model simulations. Field measurements have traditionally used sample surveys and distributed observations of above-ground and soil biomass (Fan et al., 2012). The expenses and technical requirements of this method preclude its use over wide areas and longer time intervals. Meanwhile, NPP model simulation methods generally use one of three approaches. The models themselves are referred to as climate-related statistical models (statistical methods), light energy utilization models (parametric models), and physiological and ecological process models (mechanistic models) (Zhu et al., 2005). Each model type carries with it advantages and drawbacks. Climate models produce results with relatively high uncertainty terms because they do not consider vegetation-related information (Zhou et al., 1995). Light energy utilization models include light energy transfer and conversion processes, but these remain somewhat uncertain (Field et al., 1995). Process models require many parameters that are either uncertain or difficult to obtain (Wang et al., 2002). Mechanistic models are complex and may use inaccurate assumptions. While uncertainties also affect NPP modelling approaches, researchers adopt these due to their better coverage and greater scope relative to traditional field surveys. NPP modelling can effectively constrain the understanding of regional ecological health (Li et al., 2021). Due to its utilization of satellite remote sensing technology, the CASA model has been widely used in estimating NPP in terrestrial ecosystems and in global carbon cycle research. The CASA model uses vegetation photosynthetic processes and light energy utilization as a basis (Fyllas et al., 2017) for estimating dynamics and spatiotemporal variability in NPP at the regional and global scales (Potter et al., 1993).

For mining areas, NPP can be used as a unified scale standard to measure the changes to the ecological environment in mining areas. By accurately estimating the biomass in the mining area, the spatial pattern, changing trend characteristics and response to climate change of vegetation NPP can be quantitatively analyzed, thereby reflecting the ecosystem health of the mining area. Monitoring variation in vegetation NPP can expand the understanding of the effectiveness of restoration and mitigation strategies. The results are of great significance for understanding the mechanisms of the effect of climate change on the vegetation change process in the terrestrial ecosystem in the mining area, the ecological restoration of the mining area, and effective governance (Zhang et al., 2020).

Researchers have adopted a range of model approaches for studying vegetation or other ecological parameters in coal mining areas (Hao et al., 2011; Sun et al., 2019; Kishore et al., 2016; Wang et al., 2016; Kang et al., 2014). Additionally, the research mainly focuses on analyzing the relationship between the temporal and spatial variation

characteristics of NPP and coverage in mining areas and their influencing factors. For example, Hao Chengyuan and other scholars used EOS/MODIS satellite remote sensing data to analyze the NPP of the ecosystem in the Lu'an mining area from 2001 to 2006, and conducted research and analysis from the perspective of time and space. Human activities such as farming are closely related, and the spatial heterogeneity is mostly related to natural factors such as annual precipitation. However, combined with domestic and foreign research, few studies have addressed NPP in the Shendong mining area, and very limited historical data are available. At the same time, the Shendong mining area (Ordos) area mostly involves mechanized underground mining. Compared with other mining areas, studying the changes in the surface vegetation NPP can provide corresponding research reference for other mining concentrated mining areas.

This study used the CASA model to simulate the spatio-temporal dynamics of the vegetation NPP in the Shendong mining area of Inner Mongolia from 2000 to 2019. The study also analyzed climate factors to determine both the qualitative and quantitative aspects of environmental health in Shendong. The results can help inform mitigation and restoration strategies and promote the sustainable and scientific development of the land and its resources.

2. Materials and methods

2.1. Study area

The study area is located within the broad northward arc of the Huang He River, in a zone between the Ordos Plateau and the northern edge of the northern Shanxi Plateau. To the north lies a transition zone abutting the Maousu Desert and to the south lies an eastern section of the northern edge of the Loess Plateau in northern Shanxi (Shao et al., 2022). As a typical hill and gully terrain, most of the area consists of sand dunes and other arid climate landforms. The terrain gradually increases in elevation from southeast to northwest with a series of higher-elevation drainage divides occurring roughly in the middle of the study area. The elevation ranges from 1200 to 1400 meters. The climate is categorized as a middle temperate continental climate. The winter is long and cold and the summer is hot and short. Temperatures in spring and autumn change sharply. The relatively low annual rainfall is typically discretely concentrated and the annual rainy season varies greatly. Rain depends on seasonal winds from the south in the summer, from the east in late autumn, and from the northwest in early spring. The annual average precipitation in the area is 320~400mm, and the inter-annual variation of precipitation is great. The precipitation in wet years is about 3 times that in dry years. The annual distribution is uneven, and the precipitation is small and concentrated, mainly in June to September, accounting for about 3/4 of the whole year, mostly in the form of heavy rain, with strong bursts. The annual average temperature is 7.3 °C, the annual extreme maximum temperature is 38.8 °C, and the annual extreme minimum temperature is -28.1 °C. The surface of the study area is mostly hard-beamed land with low organic matter content. The soil texture is sandy soil or sandy loam, the soil mechanical composition is coarse, and the soil texture is loose. The vegetation in the area is arid-semi-arid grassland vegetation, sandy plants dominate, and the vegetation coverage is low.

As shown in Figure 1, the study area includes 87 subsurface coal mines, including the Liuta Coal Mine, Shangwan Coal Mine and so on. Combined with the current situation of the study area, a direct impact area of well mining and a natural recovery area are set up in the study area. The geometric centers of the two areas have a difference of 29′1" in longitude, 10′05" in latitude, and a distance of 4.7 km between the geometric centers. They are both hill and gully landforms, and have the same geological origin, with similar elevations and similar slopes.

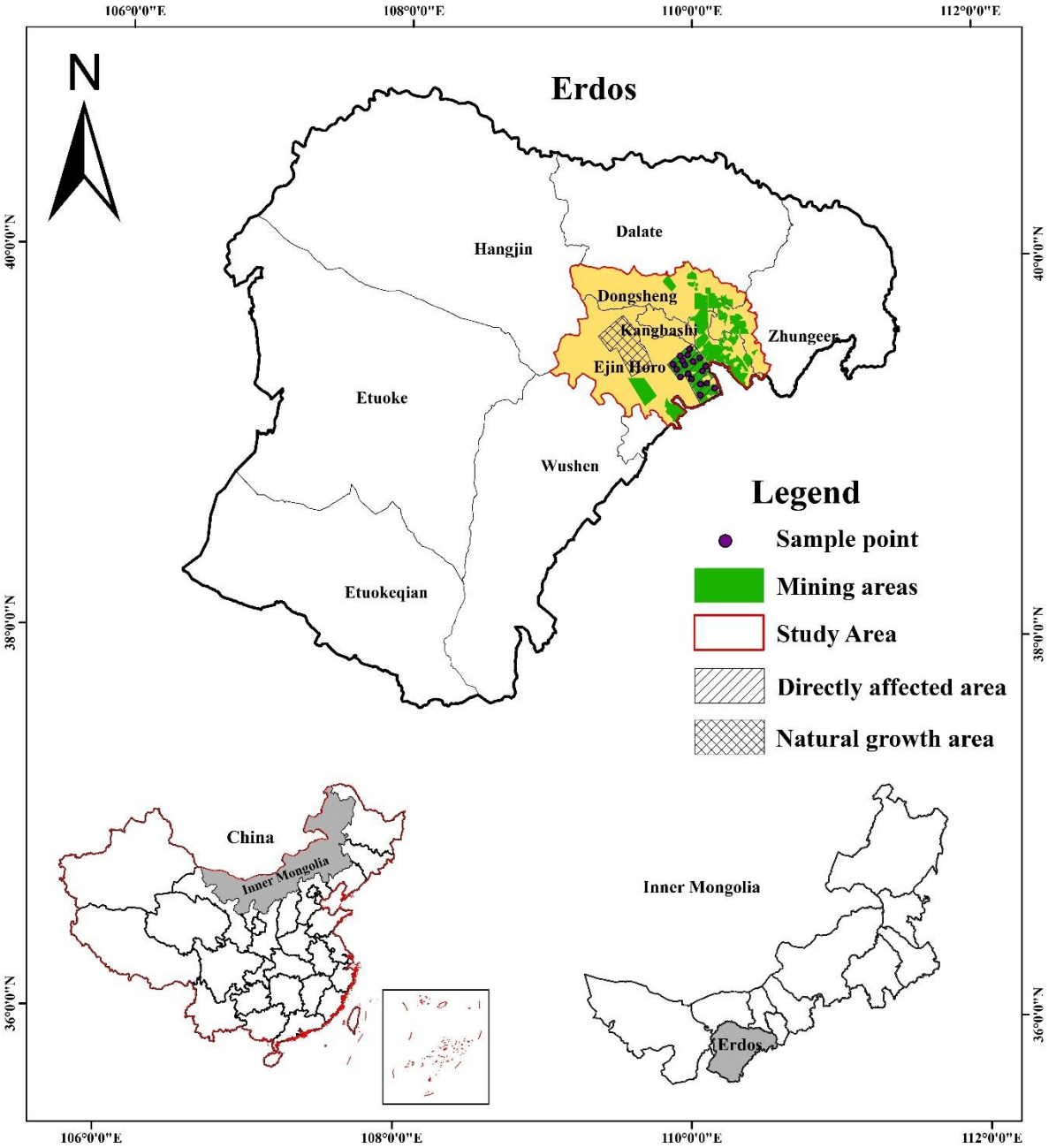

Figure 1. Overview of the study area

2.2. Data sources

2.2.1. Remote sensing data

This study used NDVI (MOD13Q1,250m, 16d) and NPP data (Zhao et al., 2005) (MOD17A3,1Km, 1a) downloaded from U.S. National Aeronautics and Space Administration (NASA) websites. The MODIS Reprojection Tool was used to convert (Geo TIFF) and reproject (WGS84/Albers Equal Area Conic) the two datasets. Monthly NDVI datasets for the study period were integrated with annual NPP data using batch methods (Han et al., 2019) to obtain MODIS NPP and NDVI time series covering the study area for the duration of the study period (2000–2019).

2.2.2. Measured NPP data

Due to the challenges and limitations posed by measuring NPP in the field, biomass conversion NPP data are usually used instead of field NPP data for data model validation. This research measured biomass in 19 plots representing the topography of the study area from July to August 2021. Considering the diversity of vegetation types in the study area, 25 × 25 m was selected as the large plot. In these areas, three 1 x 1 m grassland plots were selected for biomass sampling, and the average value was later taken as grassland biomass.

Biomass was collected, weighed immediately, labeled and transported back to the laboratory for analysis. In the lab, biomass dry weight data were obtained after samples were dried at 75 °C for 12 hours. NPP was estimated from each sample square as the proportion of above-ground biomass relative to below-ground biomass, assuming a NPP conversion coefficient of 0.475 (Li et al., 2021). Trees within large plots included sand willow and poplar trees. We counted the number of trees in each plot and estimated the size of each individual from its diameter at 1.3 m above the ground. Biomass and corresponding NPP of the forested land was estimated according to the algorithm proposed by Fan Wenyi and others (Fyllas et al., 2017). Finally, the coverage of grassland and trees was integrated into the total NPP area of each plot. NPP per unit area was determined by combining the area of the large square.

2.2.3. Meteorological data

Meteorological data were obtained from the China Meteorological Science Data Sharing Service Network (http://cdc.cma.gov.cn). The daily data of precipitation and temperature from 2000 to 2019 were collected from six standard meteorological stations in the study area and its surrounding areas. After calculating monthly precipitation and average temperature data by means of summing and averaging methods, we used ANUSPLIN to break the data into a grid to match the projection for the study area and resolution of NPP data.

2.2.4. Other data

Administrative division data came from the Inner Mongolia Autonomous Region Territorial Space Planning Institute. Vegetation cover data were obtained from the European Space Agency (https://maps.elie.ucl.ac.be/CCI/viewer/) (Guang et al., 2019). Distribution maps of subsurface mines came from the Inner Mongolia Geological Survey Planning Institute.

2.3. Methods

2.3.1. Optical Energy Utilization Model (CASA model)

The Carnegie-Ames-Stanford Approach (CASA) is a light energy utilization model proposed by Potter in 1993. This model is a mechanistic model that estimates vegetation NPP based on the vegetation's physiological processes. Meteorological data inputs include solar radiation, temperature, and precipitation. Remote sensing data inputs include the vegetation index and empirical data such as maximum light energy utilization. The model uses these to estimate the maximum primary productivity of vegetation. The present study utilized a modified CASA model (Li et al., 2009). The specific NPP formula was:

$$\mathrm{NPP}(x,t) = \mathrm{APAR}(x,t) \times \varepsilon(x,t) \quad (1)$$

where $\mathrm{APAR}(x,t)$ represents the effective photosynthetic radiation absorbed in pixel x during month t. The term $\varepsilon(x,t)$ represents the actual optical energy utilization rate of pixel x during month t.

The formula used to calculate photosynthetically active radiation was:

$$\mathrm{APAR}(x,t) = \mathrm{SOL}(x,t) \times \mathrm{FPAR}(x,t) \times 0.5 \quad (2)$$

where $\mathrm{SOL}(x,t)$ represents the total solar radiation (MJ/m^2) of pixel x during month t. The term $\mathrm{FPAR}(x,t)$ represents the vegetation's absorption ratio of photosynthetically

active radiation and the constant 0.5 indicates the proportion of effective solar radiation to total solar radiation.

The actual light energy utilization rate was calculated as:

$$\varepsilon(x,t) = f_1(x,t) \times f_2(x,t) \times W(x,t) \times \varepsilon_{max} \quad (3)$$

where $f_1(x,t)$ and $f_2(x,t)$ represent the effect of high and low temperatures on the light energy conversion rate. The term $W(x,t)$ indicates the influence of water conditions on the light energy conversion rate and ε_{max} represents the maximum light energy utilization of vegetation in the ideal state. For ε_{max}, the research results of Professor Zhu Wenquan are cited in this paper (Zhu et al., 2007).

2.3.2. Theil–Sen Median trend analysis with the Mann–Kendall non-parametric test

This study used statistical methods with good associative properties to determine trends in long-term data series. The Theil–Sen Median (sen) is a robust, nonparametric trend calculation method. Often used in trend analysis of long-term data series (Zhang et al., 2021), the method is computationally efficient and insensitive to measurement errors and outlier data. The method does not require the data to obey a certain distribution, nor does it amplify error. The formula for the trend estimation is:

$$\text{slope} = \text{median}\left(\frac{NPP_j - NPP_i}{j-i}\right), 2000 \le i < j \le 2019 \quad (4)$$

where the size of the slope term indicates the trend in vegetation with NPP> 0 for an upward trend and <0 for a downward trend.

The Mann–Kendall test is a non-parametric statistical test (M-K) originally proposed by Mann in 1945 and then further improved by Kendall and Sneyers. The M-K test does not require measurements to obey a normal distribution or linear trend. Missing values and outliers do not strongly affect results. The test is widely used in the trend analysis of long-term data series to evaluate the significance of vegetation NPP trends. The test statistic S is calculated as:

$$S = \sum_{j=1}^{n-1} \sum_{i=j+1}^{n} sgn\left(NPP_j - NPP_i\right) \quad (5)$$

where the term sgn represents a symbolic function calculated as:

$$sgn\left(NPP_j - NPP_i\right) = \begin{cases} 1 & NPP_j - NPP_i > 0 \\ 0 & NPP_j - NPP_i = 0 \\ -1 & NPP_j - NPP_i < 0 \end{cases} \quad (6)$$

The test statistic Z was used for the trend test as follows:

$$Z = \begin{cases} \frac{s}{\sqrt{Var(s)}} & S > 0 \\ 0 & S = 0 \\ \frac{s+1}{\sqrt{Var(s)}} & S < 0 \end{cases} \quad (7)$$

The function Var was calculated as:

$$Var(s) = \frac{n(n-1)(2n+5)}{18} \quad (8)$$

where n is the number of data in the sequence.

For a given confidence interval (significance level) α, absolute values of Z equal to or exceeding 1.65, 1.96, and 2.58 give respective significance levels of 90%, 95%, and 99%. If $|Z| \ge Z_{1-\alpha/2}$, the assumption of an upward or downward trend cannot be rejected (the null hypothesis is not obtained). Positive values indicate an upward trend, and negative values indicate a downward trend. According to the t-test cutoff value, when $|Z| > 1.65$, the increasing or decreasing trend is weakly significant at the 0.1 level. When $|Z| > 1.96$, the increasing or decreasing trend is significant at the 0.05 level. When $|Z| > 2.58$, the increasing or decreasing trend is extremely significant at the 0.01 level.

2.3.3. Partial correlation analysis

Both multivariate and partial correlation coefficients were calculated. The multivariate correlation coefficient was calculated as follows:

$$r_{xy} = \frac{\sum_{i=1}^{n}[(x_i-\bar{x})(y_i-\bar{y})]}{\sqrt{\sum_{i=1}^{n}[(x_i-\bar{x})^2\sum_{i=1}^{n}[(y_i-\bar{y})^2]}} \quad (9)$$

where r_{xy} represents the correlation coefficients for the x and y time series. The x_i term represents NPP and y_i represents the average temperature or precipitation in year i over a total of n years. The term $\bar{x}$ represents annual average NPP, and $\bar{y}$ represents average annual temperature or precipitation.

Partial correlation coefficients between NPP and temperature and NPP and precipitation were calculated by using pixel-based spatial analysis and the following formula:

$$R_{jkl} = \frac{R_{jk}-R_{jl}R_{kl}}{\sqrt{\left(1-R_{jl}^2\right)+(1-R_{kl}^2)}} \quad (10)$$

where R_{jkl} represents the partial correlation coefficient between variable j and variable k after variable l is fixed. The terms $R_{jk}, R_{jl}, and\ R_{kl}$ are correlation coefficients for the variables j and k, j and l, and k and l, respectively.

2.3.4. Residual analysis of multiple regression results

The analysis also used a multiple regression residual analysis method proposed by Evans and Geerken (Mike et al., 1999; Hao et al., 2018). Multiple linear regression models were used to fit the vegetation NPP according to the variation in meteorological factors. Differences between fitted and observed vegetation NPP were treated as an artificial factor to constrain the impact of climate change and human activity on changes in vegetation cover (Deng et al., 2018). The calculation ran as follows:

$$\varepsilon = NPP_{real} - NPP_{pre} \quad (11)$$

where ε is the residual error, $\varepsilon > 0$ indicates positive effects of human activity, $\varepsilon < 0$ indicates negative effects of human activity, and $\varepsilon = 0$ indicates negligible effects of human activity. The term NPP_{real} represents the observed vegetation NPP, while NPP_{pre} represents the predicted NPP.

2.3.5. Partial least-squares regression method (PLS)

Modeling by partial least-squares regression method (Wang et al., 2000) combines the advantages of principal component analysis and multivariate regression. This method used a variable projection importance discrimination index (VIP) value calculated (Perez-Enciso and Tenenhaus., 2003) as:

$$VIP_j = \sqrt{N\sum_{i=1}^{n}\sum_k R^2(y_k,t_i)w_{ij}^2 / \sum_{i=1}^{n}\sum_k R^2(y_k,t_i)} \quad (12)$$

where N represents the number of independent variables, and k is the single dependent variable. The term $R^2(y_k,t_h)$ represents the determination coefficient for both y_k and t_h, n is the number of components, t_i is the ith component of the independent variable, y_k is the kth component of the response variable, and w_{ij}^2 represents the contribution of each independent variable pair, t_h. The independent variable of VIP> 1 is generally interpreted as representing a significant explanation for the dependent variable. For 0.8 <VIP <0.8, VIP is taken to carry no explanatory significance. Otherwise, the larger the VIP value, the greater its explanatory significance.

3. Results

3.1. Model validation

Spatial comparison of observed data with the data generated by the CASA model provided a means of evaluating accuracy. Figure 2 shows the results of the correlation analysis of observed and simulated NPP, for which R^2 = 0.55 (P <0.01). The observed NPP data apparently agree with modeled data.

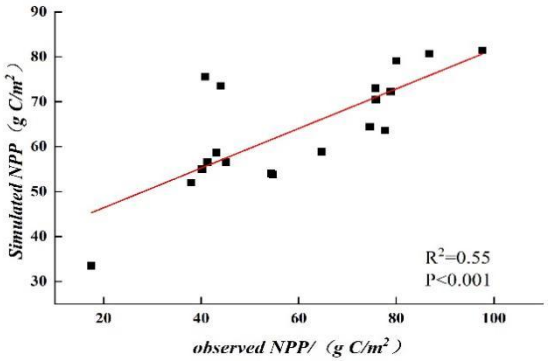

Fig. 2. Comparison between simulated and observed NPP

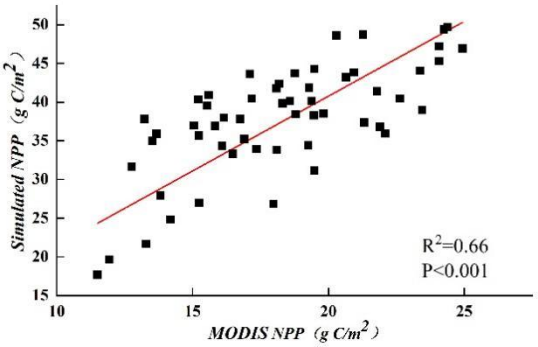

Fig. 3. Comparison between simulated and Modis NPP

Given the temporal mismatch between the model study period and the timing of observed data acquisition, we also used MODIS NPP finished product data to further validate the model data. For this procedure, 55 sample points within the study area were randomly selected for fitting analysis. As shown in Figure 3, the R^2 estimated between the MODIS NPP product value and the modeled value was 0.66 ($P < 0.01$). This indicates a high degree of consistency and that CASA can generate reasonably accurate estimates of NPP. It can better reflect the spatial distribution and interannual variation of NPP in Shendong mining area, and the simulation results have better accuracy than product data.

3.2. Spatiotemporal distribution of NPP in the Shendong mining area

According to the monthly NPP data simulated by CASA model, the total value of NPP over the time period was obtained, and then the average value of NPP in the study area was taken as the annual value of NPP over the time period. As shown in Figure 4, vegetation NPP generally fluctuated between 2000 and 2019, with slower increases in 2000–2011 and faster increases in 2011–2019. The annual average NPP over the entire study period was 44.51g C/m^2 a. The propensity rate was 1.06/a with a multiannual mean trough year in 2011 and a peak in 2018 ($P < 0.01$). These values differed by 37.04 g C/m^2 a. Annual average NPP distributions appear to have generally increased in the study area (Figure 5). Regional NPP estimates were divided into five categories using a natural fracture method. The average annual NPP for the entire region was 40 to 60 g C/m^2 a. This value represented 57.96% of the entire study area (the largest proportion). An additional 34.12% of the study area shared 20 to 40 categories, and 0.28% (minimum category) shared >80 categories.

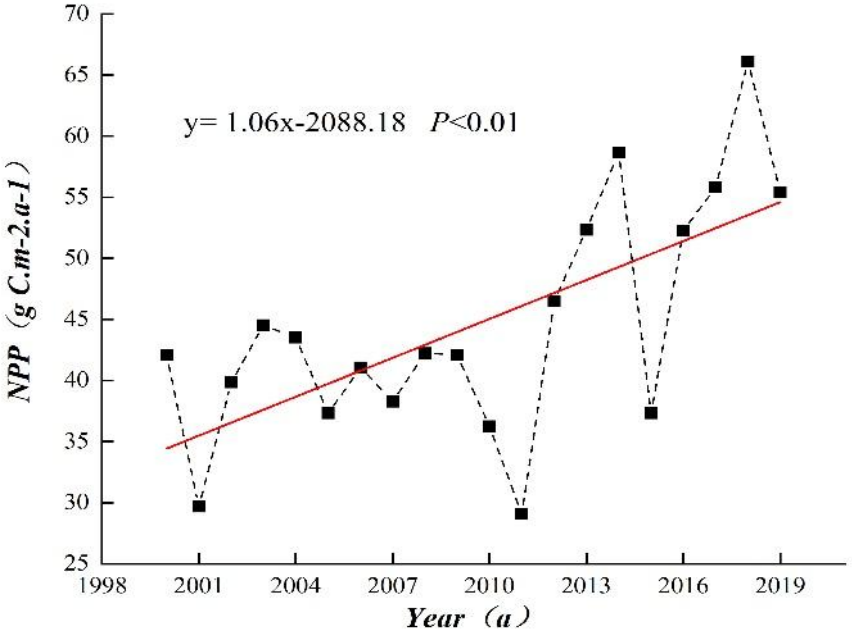

Figure 4. Interannual variation in NPP for study area from 2000-2019.

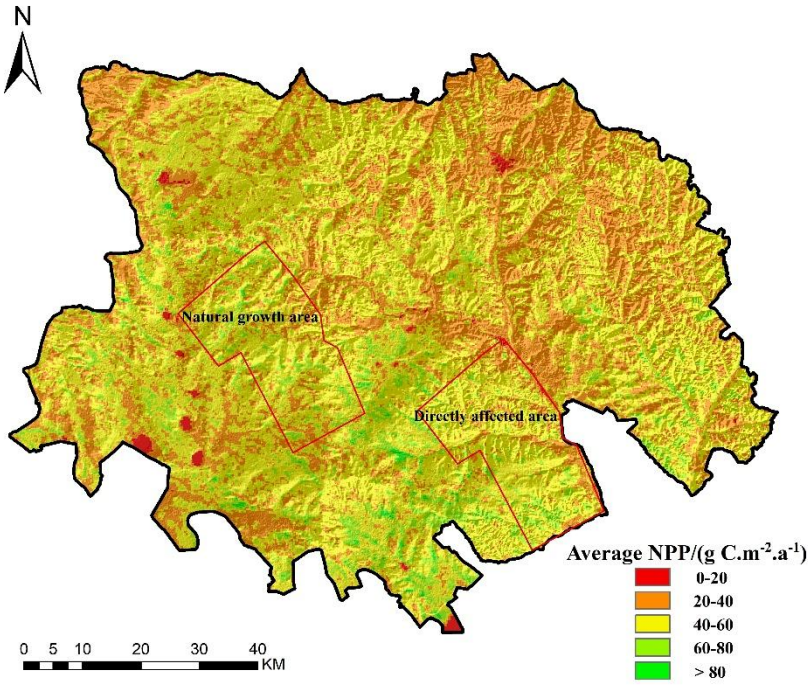

Figure 5. Spatial distribution of 20 year average NPP in study area.

Based on the NPP simulation results from 2000 to 2019, this paper used the R language to conduct Sen+MK trend analysis, and combined it with slope value division to determine the NPP trend of the study area from 2000 to 2019. As shown in Figure 6, the multi-decadal trends in NPP show considerable spatial heterogeneity. The areas of Dongsheng, Kangbashi, and Inkinhoro Banner, representing 21.54% of the study area, experienced increased vegetation NPP. Pixels representing 78.46% of the study area experienced decreasing NPP. The MK significance test (Figure 7) indicates that 1.69% of the study area experienced an extremely significant rise in NPP. Pixels representing 1.33% of the study area experienced a significant rise in NPP. Pixels representing 18.42%

of the study area experienced only a weakly significant rise in NPP. Pixels representing 0.19% of the study area experienced no significant increase in NPP. Pixels representing 0.01% of the study area experienced a very significant decline in NPP, and 0.12% of the study area experienced of significant decline in NPP. The spatial distribution of the significance of trends was consistent with that of the vegetation NPP trend itself.

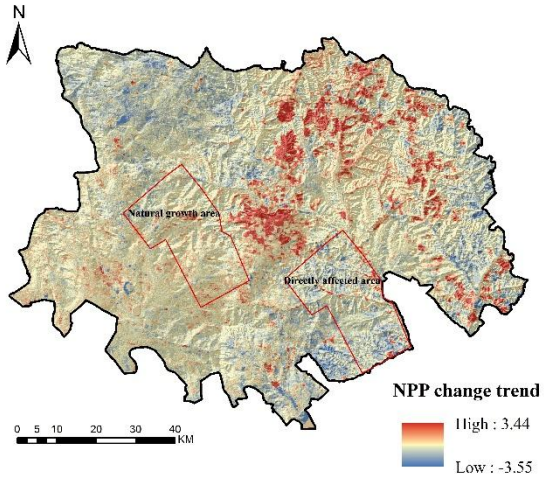

Fig. 6. Trends in NPP changes for the study area from 2000 to 2019

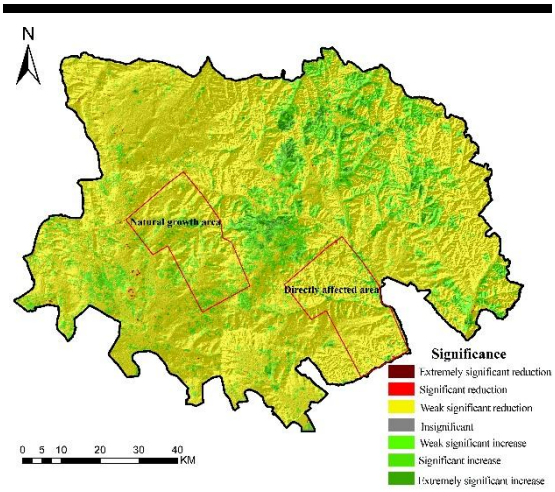

Fig. 7. Significant of interannual variation in NPP in the study area from 2000 to 2019

The direct affected area and the natural growth area in the past 20 years are listed one-to-one to determine the response law of the artificial vegetation and the natural growth area. Figure 8 shows the comparison and fitting curve of the annual NPP values between the direct affected area and the natural growth area. It can be seen that the overall net primary productivity of vegetation in both the directly affected area and the natural growth area shows a fluctuating upward trend, and the change is basically the same as that in the study area. Among them, the multi-year average value in the study period of the direct affected area is 48.26 g C/m^{-2} a^{-1}, and its tendency rate is about 1.44/a, the multi-year average value in the study period of natural growth area is 48.69 g C/m^{-2} a^{-1}, its tendency rate is about 1.12/a, and both areas pass the $P<0.01$ significance test. At the same time, it is not difficult to see that, compared with the two areas, the vegetation NPP in the area directly affected by coal mining was mostly smaller than that in the natural recovery area before 2009.

This may be related to the leap forward in development in this area from 1999 to 2009, which led to the decline of vegetation NPP in the area directly affected by coal mining.

After that, the vegetation NPP in the areas directly affected by coal mining has gradually become larger than the vegetation NPP in the natural recovery area. This may also coincide with the impact of the construction of ecological civilization proposed by China at the 17th and 18th CPC National Congress of the Communist Party of China.

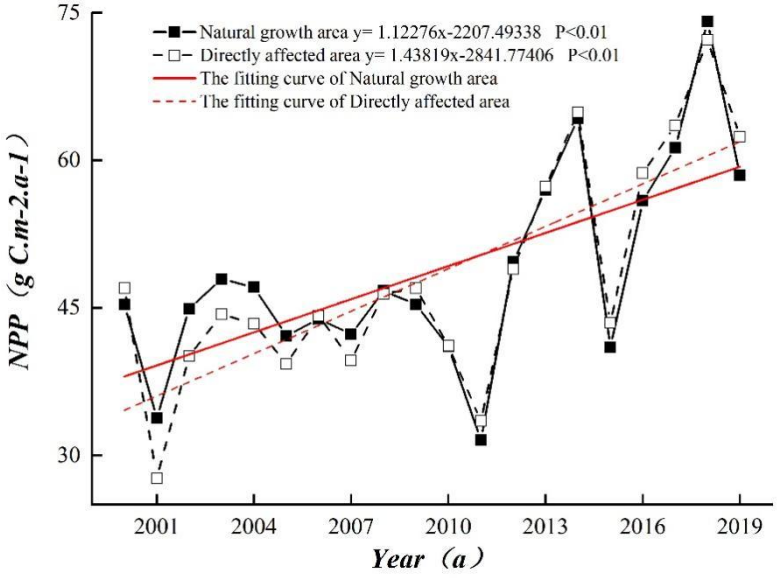

Figure 8. Change trend comparison of the NPP between the directly affected area and the natural growth area.

3.3. Meteorological factors

To determine the influence of vegetation NPP in the study area, SIMCA 14.1 was used, with annual NPP as the dependent variable and annual precipitation and annual average temperature as the independent variables. We estimated partial correlation coefficients between annual NPP and annual precipitation and average annual temperature from 2000 to 2019. As can be seen from Figure 9a,b, significant spatial differences appeared between NPP and each factor. The partial correlation coefficient for NPP and precipitation ranged from -0.60 to 0.92. The partial correlation coefficient for air temperature ranged from -0.72 to 0.77. Correlation of both factors showed both positive and negative covariance with vegetation NPP. In contrast, precipitation provided primarily positive correlation coefficients (Figure 9a). Areas positively correlated with precipitation occur primarily in the west or in scattered areas in the middle and east of the study area. These account for 92.79% of the total area. Air temperature covaried negatively with NPP (Figure 9b). Regions with negative correlation coefficients occurred primarily in western regions or distributed throughout the central and eastern regions. These represented 78.08% of the total area.

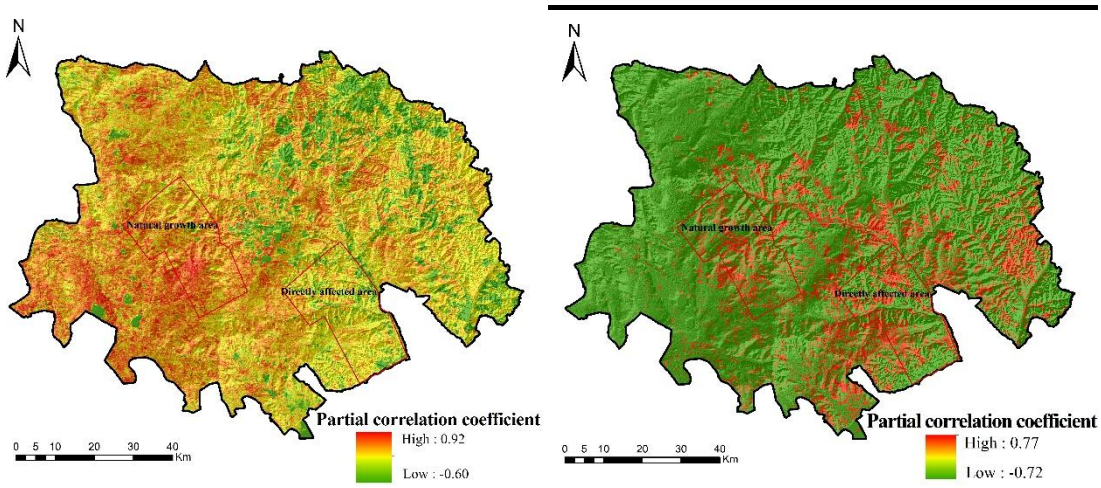

(a) precipitation **(b) temperature**

Figure 9. Partial correlation coefficients for annual average temperature and annual precipitation with NPP from 2000 to 2019.

Vegetation NPP correlated weakly with precipitation in the study area and showed significant spatial heterogeneity. The correlation coefficients between NPP and air temperature contrasted those estimated for precipitation and exhibited opposing spatial distributions. This indicates that the correlation between precipitation and temperature may jointly affect NPP.

3.4. Effects of human activity

Vegetation NPP can depend on both natural and human factors. Although climate change may influence NPP in the study area, correlation analysis can only describe the degree of covariance between NPP and various climate factors, but cannot quantify the strength of the influence. Along with climate factors, human activity may also strongly influence NPP. Residual error analysis was used to identify and quantify the influence of human activity on NPP in the study area. A multiple linear regression model based on temperature and precipitation data generated fitted NPP values for the study period. Residual estimates were obtained by calculating the difference between the predicted and observed values in the study area. Values were then analyzed as potential estimates of the influence of human activity on NPP in the study area.

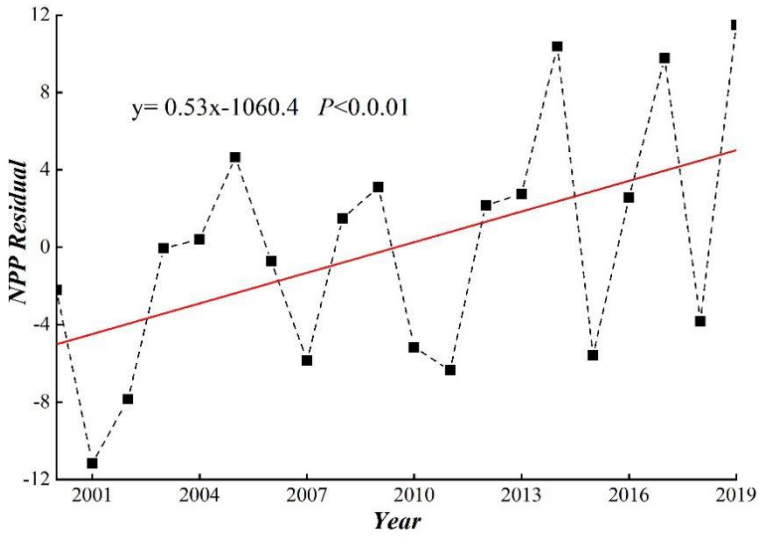

Figure 10. Interannual variation in NPP residuals for the study area from 2000-2019.

Based on the results of correlation analysis, this paper selects precipitation and temperature factors in the current year, establishes a linear regression equation based on the pixel scale to predict NPP, and obtains NPP time series with only the climate effect, so as to obtain the residual value, which is the impact of human activities on NPP. Figure 10 shows the overall trend of the estimated influence of human activity on NPP from 2000 to 2019. The trend shows a slope of 0.53 per year with considerable variation around the trend. The impact of human activity on NPP since 2011 appears relatively high in the study area. This may relate to local environmental protection efforts. Human influence on NPP from 2015 and 2018 appears relatively weak. This may relate to meteorological factors in the study area and coupling effects. Figure 11 shows the spatial distribution of the influence of human activity. Negative values indicate the influence of human activity on NPP. Only a very limited area experienced a negligible influence of human activity on NPP. The area where human activity appeared to have enhanced NPP accounted for 90.86% of the total study area. Intuitively, coal mining areas show greater human activity influence than other areas.

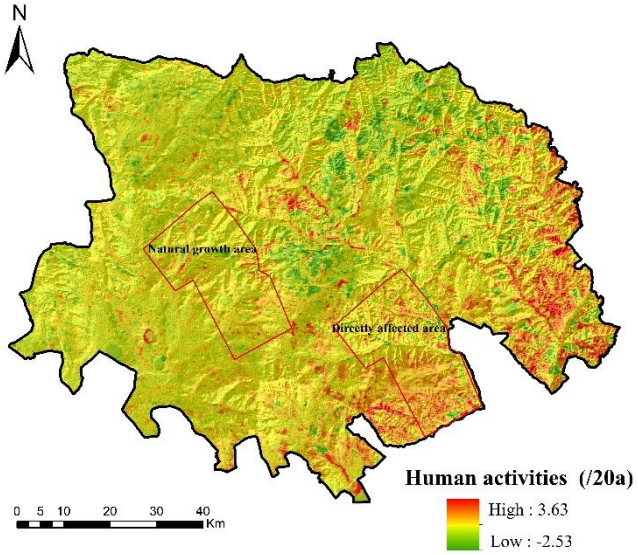

Figure 11. Spatial distribution of human activities in the study area from 2000-2019.

3.5. Double impact effects

Partial least squares analysis was used to address multivariate commonality problems arising from intercorrelated variables (Hou et al., 2015). As shown in Figure 12a, the ability of variables to explain changes in NPP (VIP) ranked as follows: human activity (1.64)> temperature (0.48)> precipitation (0.27). This indicates that human activity explains more variation than climate variation does, especially in recent years. Temperature appears to exert a stronger influence than precipitation on vegetation NPP. Figure 12b gives regression coefficients for the estimated regression equation of $y = 0.024x_1 - 19.44x_2 + 8.06x_3 + 181.97$. The terms x_1, x_2, and x_3 indicate precipitation, air temperature, and human activity. As seen in Figure 12c, air temperature exerts a negative effect on NPP, while other factors, including human activity, exert a strong positive effect indicated by an increase in NPP. These relations suggest that recent interventions promoting NPP have succeeded.

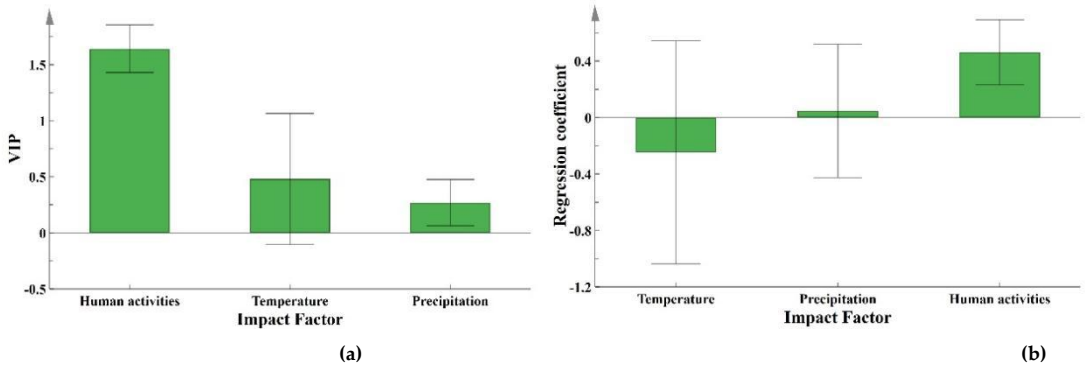

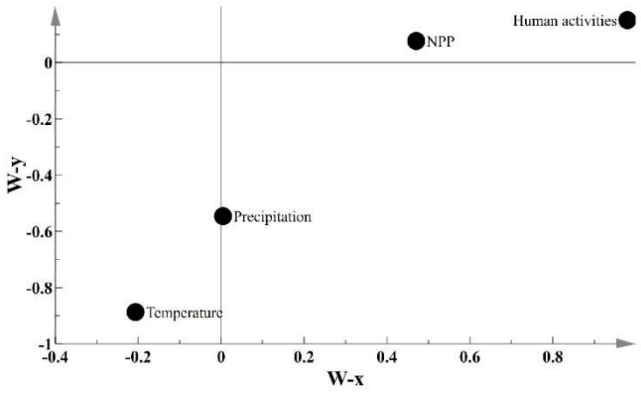

(c).

Fig. 12. PLS analysis of the influence of climate change and human activity on NPP in the study area

4. Discussion

4.1. NPP simulation results

Although the CASA model appears to have provided adequate NPP estimates for the study area, uncertainties in observed NPP and the resolution of the data may pose difficulties. Further validation of the CASA NPP can help increase confidence in the estimated results. Estimates of NPP for this region were therefore compared with previously generated CASA-generated NPP results as reported by Zhu Wenquan (Zhu et al., 2007). The results described here also generally resemble those published by Mu Shaojie (Mu et al., 2013), who performed an inversion of CASA results from the Inner Mongolia Autonomous Region (Zhu et al., 2005). The results interpreted here are generally lower than those reported by Xie S.S (Xie et al., 2015), who used a BLOME-BGC model. The differences among the inversion results may arise from several sources. Mismatched time intervals or spatial scale may generate different results. Differences in the models themselves, their parameters, or inversion settings may also cause variation. Different interpolation methods applied to data and differing scopes of the study area can introduce uncertainties into meteorological data, which propagate into spatial results. This study compared NPP results among field observational sources, model sources, and from previous sources. The results are generally consistent. Previous research has shown that the CASA model performs NPP inversion, but the current spatial resolution and temporal duration of data remain limited. The study area is also covered by only a limited number of meteorological stations. Together, these factors limit the scope of the study to analysis of only a few factors exerting potential influence on NPP.

4.2. NPP distribution and influence factor response

Studies have documented the considerable restoration of vegetation since 1980 throughout China, and especially in northern China. Although spatially heterogeneous, restoration appears to have occurred relatively rapidly (Jin et al., 2020). The present study detected obvious spatial heterogeneity at regional and local scales. The spatial heterogeneity arises largely due to human activities. The research area covers urban and developed areas such as Dongsheng District and Kangbashi. In recent years, urban development and expansion has included installation of more green space and urban landscaping. Relative to surrounding areas, results may underestimate NPP values due to lower original vegetation coverage values. Impacts associated with urban expansion and mining, including destruction of vegetation, can gradually diminish vegetation NPP for surrounding areas. Many researchers studying NPP changes have found that they

jointly depend on human activity and climate. Climate data presently record the rapid rise in temperatures (Jin et al., 2018). This can increase the release of soil organic matter and exert catalytic effects on the growth of vegetation (Li et al., 2017). Human activities such as returning farmland to forest or other ecological restoration efforts can increase vegetation coverage and productivity (Xin et al., 208). All of these factors can increase NPP. By contrast, climate change and human activity can also limit vegetation growth or coverage. Rapid warming and drying in the northwest, for example, likely intensifies drought, which limits the growth of vegetation in the region. The intensification of human activities in woodland, grassland, and other types of vegetated areas can also reduce productivity through reduced biodiversity or other impacts on the ecosystem.

As for the areas directly affected by coal mining and the natural growth areas involved in this study, the literature shows that by the end of 2019, the Shendong mining area had invested a total of 269 million yuan in ecological environment construction (Yang, K.X., 2021). The vegetation NPP in the affected area increases year by year and gradually surpasses the natural restoration area. However, as shown in this study, from the perspective of vegetation NPP over the years, under the premise of continued coal mining in the future, the vegetation ecological restoration in the area directly affected by coal mining will still be affected. Further strengthening is required.

In the area considered by this study, regional annual precipitation, temperature, and human activity all increased simultaneously over the past 20 years. The data plotted in Figures 4, 10, and 13 show that in 2014 and 2018, NPP remained high during the respective peaks of human activity and precipitation. These years experienced moderate average temperature values. This suggests that climate change and human activity can strongly influence regional NPP and its spatial distribution. Air temperature appears to covary negatively with NPP, while other factors covary positively. Human activity exerts the strongest positive influence, indicating that increases in NPP reflect effective recent human environmental interventions, including restoration.

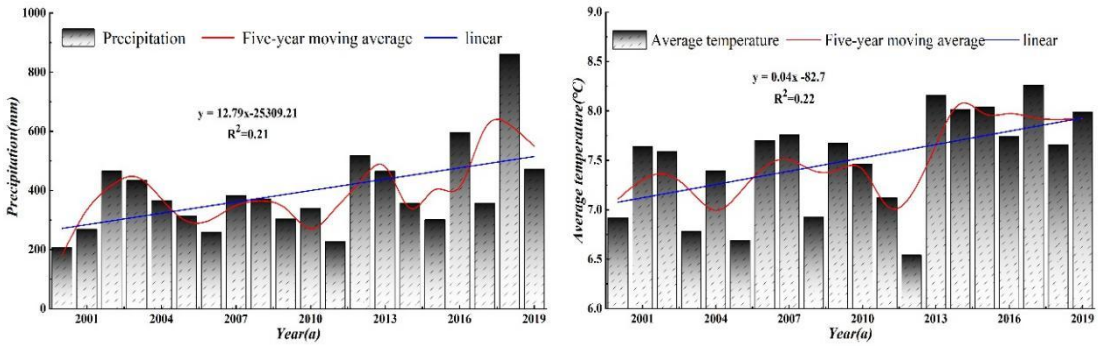

Fig. 13. Variation trends, linear trend, and 5-year moving average of precipitation and average temperature in the study area from 2000 to 2019

Accelerated urbanization of Dongsheng District, Kangbashi District, and Ejin Horo Banner undeniably reflects intensified human activity, but the effects of this activity on NPP have gradually weakened. The Shendong mining area occurs in an ecologically fragile area. Large-scale mining and human activity have included perennial vegetation restoration and irrigation with recovered water. The local environment has been negatively impacted, but mitigation efforts have reduced some of the damage. Economic development and environmental plans suggest coordinated development of "underground factory and ground gardens" as research objectives (Wang et al., 2007). Future research should further quantify and evaluate how to optimize vegetation NPP according to factors that can improve environmental quality of the area.

5. Conclusions

Through the analysis of the annual vegetation NPP and its influencing factors in the Shendong mining area from 2000 to 2019, the following conclusions can be drawn.

(1) From 2000 to 2019, the overall condition of the net primary productivity of vegetation in the study area showed a fluctuating upward trend. The multi-year average was 44.51g C/m^{-2} a^{-1}, and the trend rate was 1.06/a. The multi-year average trough year appeared in 2011, while the peak year appeared in 2018. Spatially, there is an increasing distribution from north to south. The variation trend has a large spatial heterogeneity, with the area with an increasing trend of vegetation NPP accounting for 21.54%, mainly distributed in Dongsheng District, Kangbashi District and the bordering areas of Yijinhuoluo Banner; other areas showed a decreasing trend, the area of which accounted for 78.46%.

(2) The change trend for vegetation NPP in the direct affected area and natural growth area over the years is basically consistent with the change in the overall vegetation NPP. Before 2009, the vegetation NPP in the area directly affected by coal mining was mostly smaller than that in the natural restoration area. After 2009, the vegetation NPP in the area directly affected by coal mining was mostly larger than that in the natural restoration area. This is related to the local mining situation and ecological restoration measures.

(3) There are obvious spatial differences in the response relationship between NPP and each factor in the study area. The correlation between the two factors and vegetation NPP is both positive and negative as a whole. Among them, the precipitation is mainly positive, and the temperature is negative. The correlation between vegetation NPP and temperature in the study area was weaker than that of precipitation.

(4) The overall influence of human activities on npp in the study area showed an increasing trend, with a tendency rate of 0.53/a. There are differences in the performance of human activity intensity in different years during the study period. Since 2011, the impact of human activities on NPP in the study area has been relatively strong. The overall impact of human activities on the net primary productivity of vegetation in the study area showed a decreasing distribution trend toward the central and northeastern regions.

(5) NPP changes in the study area are affected by both climate change and human activities. Human activities have a more significant contribution to the change in vegetation NPP than climate. The explanatory power of the influencing factors for the change in vegetation cover is ranked as follows: human activity > air temperature > precipitation.

In general, although the vegetation in the study area has been improved in the past 20 years, considering that the influence of regional climate conditions on vegetation growth is weak, it is necessary to strengthen the protection and restoration of the vegetation in the study area in order to ensure the stability of the ecological environment in the area in the future. It is suggested that the study area should improve its ecological construction in the future. Plants should be selected that can simultaneously tolerate stress from specific metals, drought, and low nutrient levels. At the same time, the mining environment management and supervision should be strengthened to ensure the stable improvement of vegetation ecological management in the Shendong mining area.

References

1. Fang, Y.; Zhang, W.Y.; Cao, J.W. Zhu, W.L. Analysis on the current situation and development trend of energy resources in china. Conservation and Utilization of Mineral Resources **2018**, 04, 34-42+47. http://doi.org/10.13779/j.cnki.issn1001-0076.2018.04.006.

2. Jiang, Z.M.. Reflections on energy issues in china. Journal of Shanghai Jiaotong University **2008**, 03, 345-359. http://doi.org/10.16183/j.cnki.jsjtu.2008.03.001.

3. Li, C.Y.; Cui, X.M.; Guo, Z.Z.; Yuan, D.B.; Hu, Q.F. Distribution of mining fissures induced fully mechanized caving mining and analysis on their evolvement characteristics. Mining Safety & Environmental Protection **2009**, 36(04), 65-68+91. https://doi.org/10.3969/j.issn.1

008-4495.2009.04.023.

4. Ge, W.; Deng, L.; Wang, F.; Han, J. Quantifying the contributions of human activities and climate change to vegetation net primar y productivity dynamics in China from 2001 to 2016. The Science of the total environment **2021**, 773, 145648-145648. https://doi.org/10.101 6/J.SCITOTENV.2021.145648.

5. Fan, Y.J.; Hou, X.Y.; Shi, H.X.; Shi, S.L. Efffect of carbon cycling in grassland ecosystems on climate warming. Acta Prataculturae Sinica **2012**, 03, 294-302. https://doi.org/10.11686/cyxb20120338

6. Zhu, W.Q.; Chen, Y.H.; Xu, D.; Li, J. Advances in terrestrial net primary productivity estimation models. Chinese Journal of Ecolo gy **2005**, 03, 296-300. https://doi.org/10.3321/j.issn:1000-4890.2005.03.014.

7. Li, C.H.; Zhu, T.B.; Zhou, M.; Yin, H.H.; Wang, Y.T.; Sun, H.; Cao, H.J.; Han, H.Y. Temporal and spatial change of net primary productivity of vegetation and its determinants in hexi corridor. Acta Ecologica Sinica **2021**. 05, 1-13. https://doi.org/10.5846/stxb2020011301 05.

8. Fyllas, N.M.; Bentley, L.P.; Shenkin, A.; Asner, G.P.; Atkin, O.K.; Diaz, S. Solar radiation and functional traits explain the decline of forest primary productivity along a tropical elevation gradient. Ecology Letters **2017**, 20(6), 730-740. https://doi.org/10.1111/ele.12771.

9. Potter, C.S.; Randerson, J.T.; Field, C.B.; Matson, P.A.; Vitousek, P.M.; Mooney, H.A. Terrestrial ecosystem production: a process m odel based on global satellite and surface data. Global Biogeochemical Cycles **1993**, 7(4), 811-841. https://doi.org/10.1029/93GB02725.

10. Zhang, R.P.; Guo, J.; Zhang, Y.L. Spatial distribution pattern of NPP of Xinjiang grassland and its response to climatic changes. Acta Ecologica Sinica **2020**, 40(15), 5318-5326. https://doi.org/10.5846/stxb201901270204.

11. Hao, C.Y.; Yang, Z.R. Net primary production and its spatial-temporal in Lu'an mining area based on MODIS data. Journal of C hina Coal Society **2011**, 36(11), 1840-1844. https://doi.org/CNKI:SUN:MTXB.0.2011-11-014.

12. Sun, Y.L.; Qian, S.; Yan, H.; Xu, L.L.; Wang, Y.; Cao, Y. Spatial-temporal dynamics of vegetation ecosystem in typical coal minin g area of Yunnan province during 2000–2018: A Case Study in Lincang. Ecology and Environmental Sciences **2019**, 28(12), 2381-2389. http s://doi.org/CNKI:SUN:TRYJ.0.2019-12-010.

13. Kishore, K.S.; Ranjan, S.S.; Kumar, M.S. Assessment of the capability of remote sensing and GIS techniques for monitoring reclam ation success in coal mine degraded lands. Journal of environmental management **2016**, 182. https://doi.org/10.1016/j.jenvman.2016.07.070.

14. Wang, X.; Ding, J.W.; Tan, K.; Li, H.D. Spatio-Temporal variation of net primary productivity of vegetation in mining areas of Y uxian and its affecting factors. Journal of Ecology and Rural Environment **2016**, (02), 187-194. https://doi.org/10.11934/j.issn.1673-4831.2016.0 2.003.

15. Kang, S.R.L.; Niu, J.M.; Zhang, Q.; Han, Y.J.; Dong, J.J.; Zhang, J. Impacts of mining on landscape pattern and primary productiv ity in the grassland of Inner Mongolia: a case study of Heidaigou open pit coal mining. Acta Ecologica Sinica **2014**, 11, 2855-2867. https:/ /doi.org/10.5846/stxb201304040603.

16. Li, W.; Chen, L.Q.; Zhou, T.J.; Zhang, K.; Li, L. Research progress of soil quality in china mining subsidence area. Coal Science and Technology **2011**, 39(05), 125-128. https://doi.org/CNKI:SUN:MTKJ.0.2011-05-038.

17. Zhao, M.S.; Heinsch, F.A.; Nemani, R.R.; Running, S.W. Improvements of the MODIS terrestrial gross and net primary productio n global data set. Remote Sensing of Environment **2005**, 95(2), 164-176. https://doi.org/10.1016/j.rse.2004.12.011.

18. Guang, X.; Bao, Z.C. Generating a series of land covers by assimilating the existing land cover maps. ISPRS Journal of Photogra mmetry and Remote Sensing **2019**, 147, 206-214. https://doi.org/10.1016/j.isprsjprs.2018.11.018.

19. Zhang, Z.Q.; Liu, H.; Zuo, Q.T.; Yu, J.T.; Li, Y. Spatiotemporal change of fractional vegetation cover in the Yellow River Basin d uring 2000-2019.Resources Science **2021**, 04, 849-858. https://doi.org/10.18402/resci.2021.04.18.

20. Mike, H.; Elaine, M.B.; Nigel, W.A.; Paula, A.H.; Timothy, C.J.; Thomas, E.D. Relative impacts of human-induced climate change and natural climate variability. Nature: International weekly journal of science **1999**, 397(6721). https://doi.org/10.1038/17789.

21. Hao, W.; Liu, G.H.; Li, Z.S.; Xin, Y.E.; Fu, B.J.; Lv, Y.H. Impacts of Drought and Human Activity on Vegetation Growth in the Grain for Green Program Region, China. Chinese Geographical Science **2018**, 28(03), 470-481. https://doi.org/10.1007/s11769-018-0952-8.

22. Deng, C.H.; Bai, H.Y.; Gao, S.; Liu, R.J.; Ma, X.P; Huang, X.Y. Spatial-temporal variation of the vegetation coverage in qinling m ountains and its dual response to climate change and human activities. Journal of Natural Resources **2018**, 03, 425-438. https://doi.org/10.1 1849/zrzyxb.20170139.

23. Perez-Enciso, M.; Tenenhaus, M. Prediction of clinical outcome with microarray data: a partial least squares discriminant analysis (PLS-DA) approach. Human Genetics **2003**, 112(5-6):581-592. https://doi.org/10.1007/s00439-003-0921-9.

24. Hou, M.T.; Hu, W.; Qiao, H.L.; Li, W.G.; Yan, X.D. Application of partial least squares (PLS) regression method in attribution of vegetation change in eastern china. Journal of Natural Resources **2015**, 03, 409-422. https://doi.org/ 10.11849/zrzyxb.2015.03.005.

25. Zhu, W.Q.; Pan, Y.Z.; Zhang, J.S. Estimation Of net primary productivity of chinese terrestrial vegetation based on remote sensin g. Chinese Journal of Plant Ecology **2007**, 03, 413-424. https://doi.org/10.17521/cjpe.2007.0050.

26. Mu, S.J.; Li, J.L.; Zhou. W.; Yang, H.F.; Zhang, C.B.; Ju, W.M. Spatial-temporal distribution of net primary productivity and its re lationship with climate factors in Inner Mongolia from 2001 to 2010. Acta Ecologica Sinica **2013**, 12, 3752-3764. https://doi.org/10.5846/stxb 201205030638.

27. Zhu, W.Q.; Pan, Y.Z.; Long, Z.H.; Chen, Y.H.; Li, J.; Hu, H.B. Estimating net primary productivity of terrestrial vegetation based on GIS and RS：A case study in inner Mongolia, China. Journal of Remote Sensing **2005**, 03, 300-307. https://doi.org/ 10.3321/j.issn:1007-4 619.2005.03.012.

28. Xie, S.S.; Ma, C.; Tian, S.J.; Tian, J.G. NPP Changes and climate impact of Shendong coalfield from 2000 to 2010. Journal of geo matics science and technology **2015**, 01, 47-51. https://doi.org/10.3969/j.issn.1673-6338.2015.01.010.

29. Jin, K.; Wang, F.; Han, J.Q.; Shi, S.Y.; Ding, W.B. Contribution of climatic change and human activities to vegetation NDVI chan ge over china during 1982-2015. Acta Geographica Sinica **2020**, 05, 961-974. https://doi.org/CNKI:SUN:DLXB.0.2020-05-007.

30. Jin, K.; Wang, F.; Yu, Q.; Gou, J.; Liu, H. Varied degrees of urbanization effects on observed surface air temperature trends in C hina. Climate Research **2018**, 76(2), 131-143. https://doi.org/10.3354/cr01531.

31. Li, J.; Liu, H.B.; Li, C.Y.; Li, Long. Changes of green-up day of vegetation growing season based on GIMMS 3g NDVI in northe rn china in recent 30 years. Scientia Geographica Sinica **2017**, 04, 620-629. https://doi.org/10.13249/j.cnki.sgs.2017.04.016.

35. Xin, Z.; Xu, J.; Zheng, W. Spatiotemporal variations of vegetation cover on the chinese loess plateau (1981-2006): Impacts of clim ate changes and human activities. Science in China Series D-Earth Sciences **2008**, 51(1):67-78. https://doi.org/10.1007/s11430-007-0137-2.

36. Yang, X.K. Coal enterprises are green. Economic Daily **2021**, 006. https://doi.org/10.28425/n.cnki.njjrb.2021.008534.

37. Wang, A. Construction and benefits of integrated measures system for environment conservation in Shengdong diggings. Science of Soil and Water Conservation **2007**, 05, 83-87. https://doi.org/10.3969/j.issn.1672-3007.2007.05.016.

38. Wang, F.; Song, Y.X.; Wang, W.G. The Empirical Study on Regional Economic Disparities and Evolution in Inner Mongolia. Econ omic Geography **2012**, 32(11):1-7. https://doi.org/10.15957/j.cnki.jjdl.2012.11.001.

39. Xiao, W.; Zhang, W.K. Spatio-temporal patterns of ecological capital under different mining intensities in an ecologically fragile mining area in Western China:A case study of Shenfu mining area. Journal of Natural Resources **2019**, 35(01):68-81. https://doi: 10.31497/z rzyxb.20200107.

40. Zhou, G.S.; Zhang, X.S. Model of net primary productivity of natural vegetation. Chinese Journal of Plant Ecology **1995**, (03):193-200. https://CNKI:SUN:ZWSB.0.1995-03-000.

41. Field C.B.; Randerson, J.T.; Malmströ m CM. Global net primary production: Combining ecology and remote sensing. Remote Sen sing of Environment **1995**, 51(1). https://doi.org/10.1016/0034-4257(94)00066-V.

42. Wang Z.M.; Liang Y.L. Progress in Vegetation Net Primary Productivity Model Research. Journal of Northwest Forestry Universit y **2002**, (02):22-25. https://doi.org/10.3969/j.issn.1005-3409.2005.03.041.

43. Shao, T.Y.; Bao, S.Q.; He, S. Spatial and temporal evolution characteristics of surface water in Shendong Mining Area based on T VDI. Journal of Northwest A & F University (Natural Science Edition) **2022**, (02):1-12. https://doi.org/10.13207/j.cnki.jnwafu.2023.02.015.

44. Han, B.H.; Zhou, B.R.; Yan, Y.Q. Analysis of Vegetation Coverage Change and Its Driving Factors over Tibetan Plateau From 200

0 to 2008. Acta Agrestia Sinica **2019**, 27(6), 1651-1658. https://doi.org/10.11733/j.issn.1007-0435.2019.06.023.

45. Yao, G.Z. Effect of coal mining subsidence on ecological environment and recovery technique. doctoral thesis. Beijing forestry uni versity. Beijing. 2012.

46. Fan, W.Y.; Zhang, H.Y. Comparison of three models of forest biomass estimation. Chinese Journal of Plant Ecology **2011**, 35(04), 402-410. https://doi.org/10.3724/SP.J.1258.2011.00402.

47. Wang, H.W.; Zhang, Q. Identification of optimal subspace from PLS regression. Journal of Beijing University of Aeronautics and Astronautics **2000**, (04), 473-476. DOI:10.13700/j.bh.1001-5965.2000.04.027.

Arabian Journal of Geosciences (2023) 16:366
https://doi.org/10.1007/s12517-023-11400-6

REVIEW PAPER

NPP spatio-temporal change characteristics and contribution analysis of land-use type in the Shendong mining area

Jia Ke[1,2] · Dandan Zhou[1] · Chunxing Hai[1] · Xiaohan Chen[1] · Bingzi Li[2] · Tang Lei[2]

Received: 26 April 2022 / Accepted: 31 March 2023

Abstract

While driving regional economic development, coal mining also causes environmental problems. Changes in land use are associated with mining impact vegetation's net primary productivity (NPP). This, in turn, can impact vegetation's carbon fixation capacity. Understanding how these impacts operate can inform vegetation restoration efforts in former mining areas and preserve ecological stability. In this paper, the NPP of the study area from 2000 to 2019 was retrieved based on the Carnegie–Ames–Stanford Approach (CASA) model, and the spatial and temporal distribution characteristics of NPP of the study area were discussed. Meanwhile, combined with the land-use data of the European Space Agency (ESA) in 2000, 2010, and 2019, the impact of land-use changes on regional vegetation NPP was discussed from the perspective of landscape ecology. The results showed that the CASA model using inverted NPP data gave results that compared favorably with data measured in the field. The annual average vegetation NPP in the study area during the study period was 44.51 g C m^{-2} a^{-1}. NPP changes showed considerable spatial heterogeneity, but the same overall trends in fluctuation. The study area experienced a decline in both forested and grassland area from 2000 to 2010. The NPP of all four land types decreased. Forested and other land types increased from 2010 to 2019, and the NPP of all four categories increased. Land-use changes over the study period of two decades promoted NPP growth, contributing 44.66% and 93.9%, respectively. Except for the aggregation index, landscape pattern indices showed a positive correlation with NPP. NPP values in 2000, 2010, and 2019 all increased, showing the highest ranked principal components based on landscape indices. The NPP in the study area strongly depends on human activities. Maintaining the current vegetation status would increase NPP in the study area and enhance the vegetation's carbon fixation capacity.

Keywords NPP · CASA · Shendong mine area · Land use · Landscape pattern index

Introduction

With the development of modern society, global land-use and cover change (LUCC) approaches have documented extensive degradation of the environment. China is a developing country, which is economically dependent on coal production and consumption. With the rapid development of the economy, coal production has caused significant changes in land use (Xu et al. 2019). Especially in arid areas, coal production has impacted regional biodiversity, soil, and other ecosystems, as reflected in the LUCC (Vadrevu et al. 2015).

The Inner Mongolia Autonomous Region is a key area for China's coal mining strategy (Hu et al. 2018). This area hosts two large national coal mines, referred to as "Mengdong" and "Mengxi." The Mengxi mining area is located in and around Ordos City, Inner Mongolia, and includes the Shendong mining area (Ordos). With its simple geological structure, Shendong consists of thick coal seams, which are suitable for large-scale subsurface mining, but the mine structures rest beneath an ecologically fragile area, subject to subsidence, collapse, and other mass wasting processes. Mining activity both provides economic benefits and has

Responsible Editor: Amjad Kallel

✉ Dandan Zhou
zhoudandan@imnu.edu.cn

Jia Ke
jiake@nmgkjghy.ntesmail.com

[1] College of Geographical Science, Inner Mongolia Normal University, Hohhot 010022, China

[2] Inner Mongolia Institute of Territorial Space Planning, Hohhot 010018, China

Published online: 12 May 2023

negative consequences for the surface environment (Li et al. 2009). The major LUCC changes reflect mines' subsidence. Over time, subsidence has also caused habitat fragmentation and other ecosystem disruptions (Xiao et al. 2010; Li et al. 2011).

In recent years, Chinese governmental policies have begun to promote environmental management and ecological restoration (Yu 2013). Mining area restoration has become a priority. Vegetation represents a key factor in the restoration of natural ecological processes (Ge et al. 2021). Restoration efforts often use net vegetation productivity (net primary production, NPP) as an indicator of ecosystem health. NPP also functions within the global carbon cycle to convert CO_2 into biomass and soil. In mining areas, changes in vegetation NPP can demonstrate the efficacy of restoration efforts and the carbon fixation capacity of plant communities that experience land-use changes (Wang et al. 2009). Vegetation NPP provides quantitative constraints on restoration and environmental management goals for mining areas (Zhang et al. 2020). The CASA model estimates NPP according to photosynthetic processes and light-energy utilization, as derived from the current understanding of plant physiology (Fyllas et al. 2017). The CASA model requires fewer input parameters than other models, so it avoids the error caused by artificial simplification or estimation due to the lack of parameters. Many researchers use CASA to assess the dynamics and spatio-temporal variability in NPP at both the global and regional scales (Potter et al. 1993). This is one of the most common NPP models in the world.

The Shendong mine mining area is one of China's main coal-generating regions, and is studied by some scholars, looking at the ecological environment. However, as environmental governance of the mines gradually strengthens, the lack of research on vegetation, especially using CASA model to look at NPP inversion in the area, has become apparent. This research used the CASA model to simulate the spatial and temporal dynamics of vegetation NPP from 2000 to 2019 in the Ordos/Shendong mining area of Inner Mongolia. The results indicate spatial and temporal patterns and constraints on vegetation productivity, given land-use changes during the study period. It is expected to provide reference for the optimization of land-use structure, improvement of vegetation carbon sequestration capacity, and sustainable scientific development in the same type of well mining area.

Materials and methods

Study area

The study area is located in the broad northward arc of the Huang He River, in the zone between the Ordos Plateau and the northern edge of the northern Shanxi Plateau. To the north lies a transition zone abutting the Maousu Desert and to the south lies an eastern section of the northern edge of the Loess Plateau in northern Shanxi. As a typical hill and gully terrain, most of the area consists of sand dunes and other arid climate landforms. The terrain gradually increases in elevation from the southeast to northwest with a series of higher elevation drainage divides roughly occurring in the middle of the study area. Elevations range from 1200 to 1400 m. The climate is categorized as a middle-temperate continental climate. The winter is long and cold and summer is hot and short. Temperatures change sharply in spring and autumn. The relatively low annual rainfall is typically discretely concentrated, and the annual rainy season greatly varies. The rain depends on seasonal winds from the south in the summer, from the east in late autumn, and from the northwest in early spring. The soil texture is sandy or sandy soil, with a coarse mechanical composition and loose soil quality. The vegetation in this area belongs to arid and semi-arid steppe vegetation, the vegetation coverage is low, and artificial vegetation accounts for a large proportion. The research area includes 87 coal mines, such as the Liuta coal mine and Shangwan coal mine (Fig. 1).

Data sources

Remote sensing data

This study used NDVI (MOD13Q1, 250 m, 16d) and NPP data (MOD17A3, 1 km, 1a), downloaded from U.S. National Aeronautics and Space Administration (NASA) websites. The MODIS Reprojection Tool was used to convert (Geo TIFF) and reproject (WGS84/Albers Equal Area Conic) the two datasets (Zhao et al. 2005). Monthly NDVI datasets for the study period were integrated with annual NPP data using batch methods to obtain MODIS NPP and NDVI time series covering the study area for the duration of the study period (2000–2019).

Measured NPP data

Due to the challenges and limitations of measuring NPP in the field, biomass conversion NPP data are often used instead of field NPP data. Field data, however, can effectively validate models. From July to August 2021, 19 plots were uniformly selected in the well-mining-concentrated areas in the study area. Through field observations of the 19 plots, the biomass measurement was carried out in the areas with intact community structure and consistent habitat conditions. The plots measured 25×25 m. Within these, three 1×1 m plots of grassland along the greater plot's diagonal were sampled for biomass. Biomass was collected,

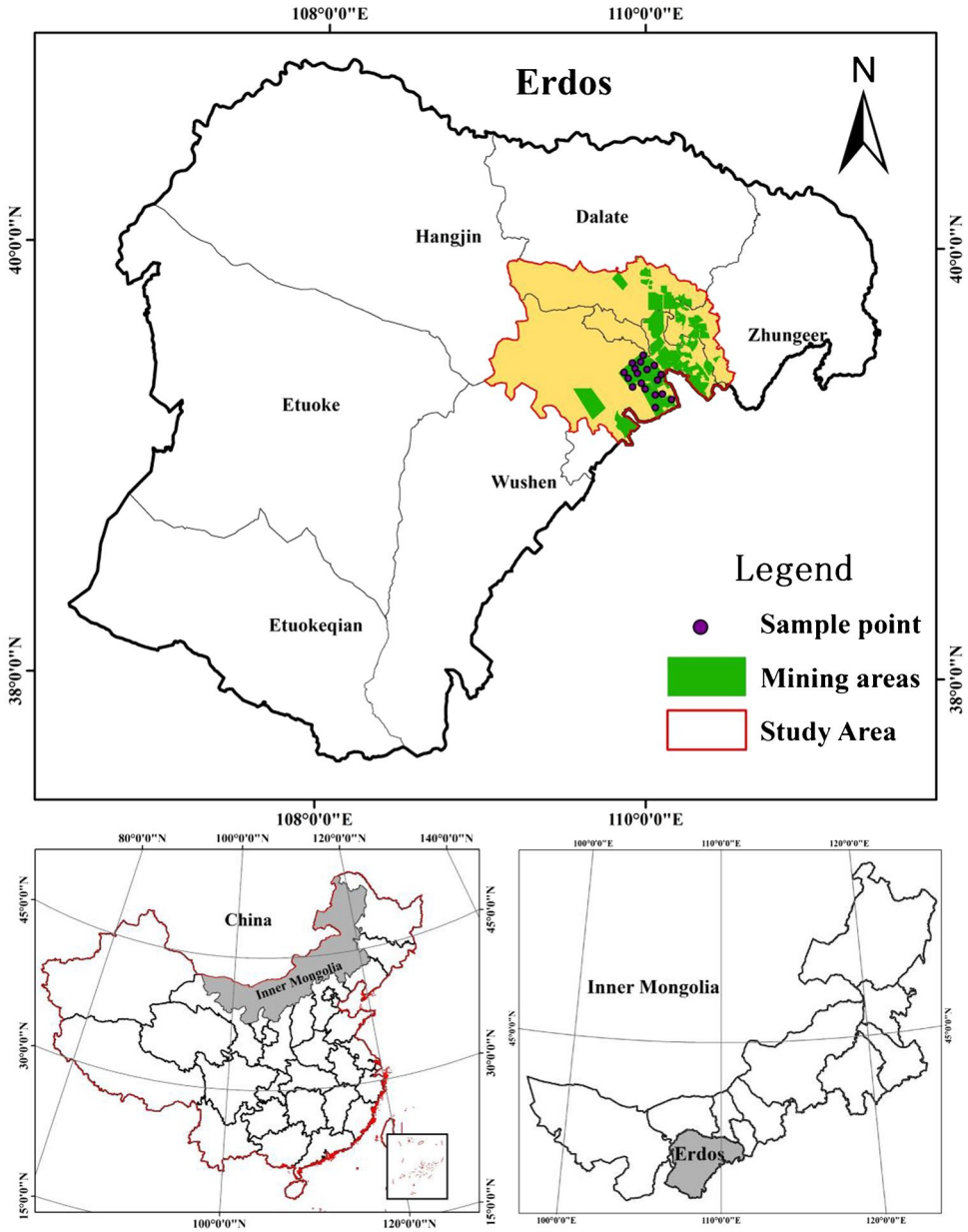

Fig. 1 Location of the study area, Inner Mongolia, China

immediately weighed, labeled, and transported back to the laboratory for analysis. In the lab, samples were dried at 75 °C to obtain biomass dry-weight data. The NPP was estimated from each sample square as the proportions of above-ground biomass relative to below-ground biomass, assuming a NPP conversion coefficient of 0.475 (Fyllas et al. 2017). The trees found in the study area include sand willow and poplars. We counted the number of trees in each plot and estimated the size of each individual from its diameter at 1.3 m above the ground. The biomass and corresponding NPP of the forested land were estimated according to the algorithm proposed by Fyllas et al. (2017). This rate, combined with forest cover, was integrated into areal estimates of total NPP per sample plot.

Meteorological data

Meteorological data were obtained from the China Meteorological Science Data Sharing Service Network (http://cdc.cma.gov.cn). Data from six standard meteorological stations within the study area and its surroundings were combined with other 2000–2019 meteorological data. Data were then parsed into a grid to match the projection for the study area and resolution of NPP data.

Land-use data

Land vegetation cover data were obtained at 300 m resolution for 2000, 2010, and 2019 from ESA (http://maps.elie.

ucl.ac.Thebe/CCI/viewer/). These were resampled at 250 m and converted to NC data using the QGIS software. The CCI-LC2000 data were converted to a standard projection and trimmed with vector boundaries. Due to the low resolution of the land-use data and the limited green space in the study area, the analysis considered only the main farmland vegetation types according to UN-LCCS, grassland, forested land, and other types (Guang and Bao 2019).

Human activity-related data

Administrative division data came from the Inner Mongolia Autonomous Region Territorial Space Planning Institute. Distribution maps of subsurface mines came from the Inner Mongolia Geological Survey Planning Institute.

Methods

Carnegie–Ames–Stanford Approach (CASA)

The CASA is a light-energy utilization model, proposed by Potter in 1993. This CASA is a mechanistic model that estimates vegetation NPP based on the vegetation's physiological processes. The meteorological data input to the model include solar radiation, temperature, and precipitation. The input remote sensing data include the vegetation index and empirical data, such as maximum light-energy utilization. The model uses these to estimate the maximum primary productivity of vegetation. As it can use satellite remote sensing technology, the CASA model is widely used to estimate NPP in terrestrial ecosystems and in global carbon cycle research. The present study utilized a modified CASA model (Zhu et al. 2005a, b). The specific NPP formula was:

$$NPP(x,t) = APAR(x,t) \times \varepsilon(x,t) \tag{1}$$

where $APAR(x,t)$ represents the effective photosynthetic radiation absorbed in pixel x during month t. The term $\varepsilon(x,t)$ represents the actual optical energy utilization rate of pixel x during month t.

The formula used to calculate photosynthetically active radiation was as follows:

$$APAR(x,t) = SOL(x,t) \times FPAR(x,t) \times 0.5 \tag{2}$$

where $SOL(x,t)$ represents the total solar radiation (MJ/m^2) of pixel x during month t. The term $FPAR(x,t)$ represents the vegetation's absorption ratio of photosynthetically active radiation and the constant 0.5 indicates the proportion of effective solar radiation to total solar radiation.

The actual light-energy utilization rate was calculated as:

$$\varepsilon(x,t) = f_1(x,t) \times f_2(x,t) \times W(x,t) \times \varepsilon_{max} \tag{3}$$

where $f_1(x,t)$ and $f_2(x,t)$ represent the effect of high and low temperatures on the light-energy conversion rate. The term $W(x,t)$ indicates the influence of water conditions on the light-energy conversion rate and ε_{max} represents the maximum light-energy utilization of vegetation in the ideal state.

Analysis of NPP's spatial and temporal characteristics

The Theil-Sen Median is a robust, non-parametric statistic. Computationally efficient and insensitive to measurement error and outlier data, the statistic is often used in trend analyses of long-term data series (Zhang et al. 2021). The method does not assume that the data follow a certain distribution, and thus minimizes error. The formula for trend analysis is as follows:

$$slope = median\left(\frac{NPP_j - NPP_i}{j-i}\right), 2000 \le i < j \le 2019 \tag{4}$$

While there is currently no standard method of parsing the slope (Zhuang et al. 2009), we sub-divided NPP changes into five grades: significant growth (slope > 5), mild growth (1 > slope < 5), stable change (−1 < slope < 1), mild reduction (−1 > slope < −5), and significant reduction (slope < −5).

The Mann–Kendall is a non-parametric statistical test (M–K) that does not require data to be normally distributed or follow a linear trend in order to function properly, and is not affected by missing values or outliers. The M–K test is widely used to determine trend significance in long-term data series. Here, it was used to determine the significance of vegetation NPP trends. The test statistic S is calculated as follows:

$$S = \sum_{j=1}^{n-1} \sum_{i=j+1}^{n} sgn\left(NPP_j - NPP_i\right) \tag{5}$$

where the term "sgn" represents a symbolic function, calculated as:

$$sgn\left(NPP_j - NPP_i\right) = \begin{cases} 1 NPP_j - NPP_i > 0 \\ 0 NPP_j - NPP_i = 0 \\ -1 NPP_j - NPP_i < 0 \end{cases} \tag{6}$$

The test statistic Z was used for the trend test as follows:

$$Z = \begin{cases} \frac{s}{\sqrt{Var(s)}} & S > 0 \\ 0 & S = 0 \\ \frac{s+1}{\sqrt{Var(s)}} & S < 0 \end{cases} \tag{7}$$

The Var function was calculated as:

$$Var(s) = \frac{n(n-1)(2n+5)}{18} \tag{8}$$

where n is the amount of data in the sequence.

For a given confidence interval (significance level) α, absolute values of Z equal to or exceeding 1.65, 1.96, and 2.58 give respective significance levels of 90%, 95%, and 99%. If $|Z| \geq Z1\text{-}\alpha/2$, the assumption of an upward or downward trend cannot be rejected (the null hypothesis is not obtained). Positive values indicate an upward trend, and negative values indicate a downward trend. According to the t-test cutoff value, when $|Z| > 1.96$, the increasing or decreasing trend is significant at the 0.05 level. When $|Z| > 2.58$, the increasing or decreasing trend is significant at the 0.01 level.

Effects of landscape changes on NPP

The pattern of changes in the research area landscape over the last 19 years was analyzed by constructing a land-use transfer matrix covering the Shendong mining area from 2000 to 2019. The effect of changes in land use on regional NPP can be expressed as the contribution of land-use change to changes in total NPP (Roc):

$$Roc = \frac{|\Delta S \times NPP_1|}{|\Delta NPP \times S_1| + |\Delta S \times NPP_1| + |\Delta NPP \times \Delta S|} \times 100\% \quad (9)$$

In Formula (9), S and NPP indicate the land-use area and NPP changes during the period, while S_1 and NPP_1 indicate initial land-use area and NPP values, respectively.

An analysis of the changes in landscape patterns was based on the previous landscape pattern index (Liu et al. 2021; Hou et al. 2020). In this paper, five indices were calculated from landscape data, including Shannon's Diversity Index (SHDI), which represents type diversity, Patch density (PD) and fractal dimension index (FRAC), which represent spatial morphology, and Splitting Index (SPLIT) and aggregation Index (AI), which represent spatial relationships. The landscape index was calculated in Fragstats 4.2 using the mobile pane method (500 m). Landscape indices and NPP values for each year were then extracted using an ArcGIS grid method. The correlation coefficients were calculated in SPSS. Variations in the five landscape pattern indices were further analyzed using principal component analysis to determine the sources of variation in NPP.

Results

Model validation

The measured NPP data were compared to the CASA model results based on spatial position to verify the model accuracy. Figure 2 shows the results of the correlation analysis of the measured data and the simulated NPP. The

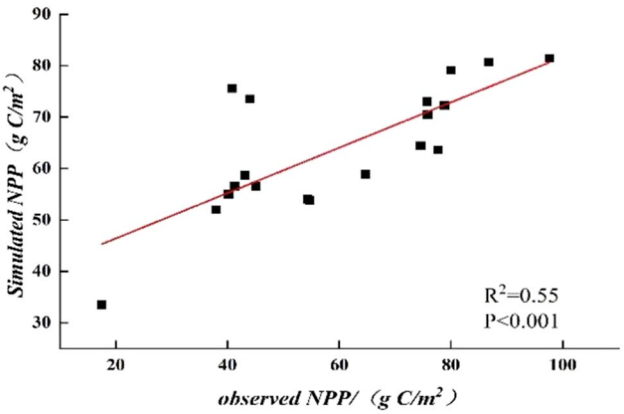

Fig. 2 Comparison of CASA simulated and observed NPP

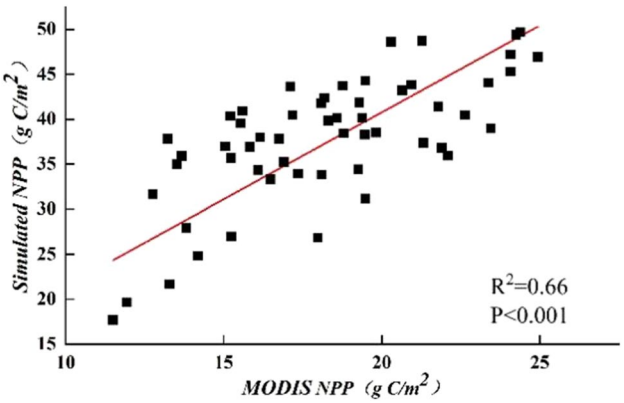

Fig. 3 Comparison of CASA simulated and Modis NPP

R^2 value of 0.55 ($P < 0.01$) indicates that the measured NPP values generally agree with the simulated values.

Due to the non-overlap of the time periods covered by the model and field (measured) data, the finished Modis NPP product data were used to further verify the model results. This method used 55 randomly selected sample points in the study area for fitting analysis (Fig. 3). The R^2 of 0.66 ($P < 0.01$) between the Modis NPP product value and the simulated value further indicates that the simulation value generally resembles the finished product value, and that the CASA model provides reasonable estimates of NPP.

NPP spatio-temporal change characteristics and contribution analysis of land-use type

As shown in Fig. 4, vegetation NPP in the study area generally increased between 2000 and 2019, with more gradual increases from 2000 to 2011 and more rapid increases from 2011 to 2019. The annual average NPP throughout the study period was 44.51 g·C·m^{-2}·a^{-1}. The propensity rate was 1.06

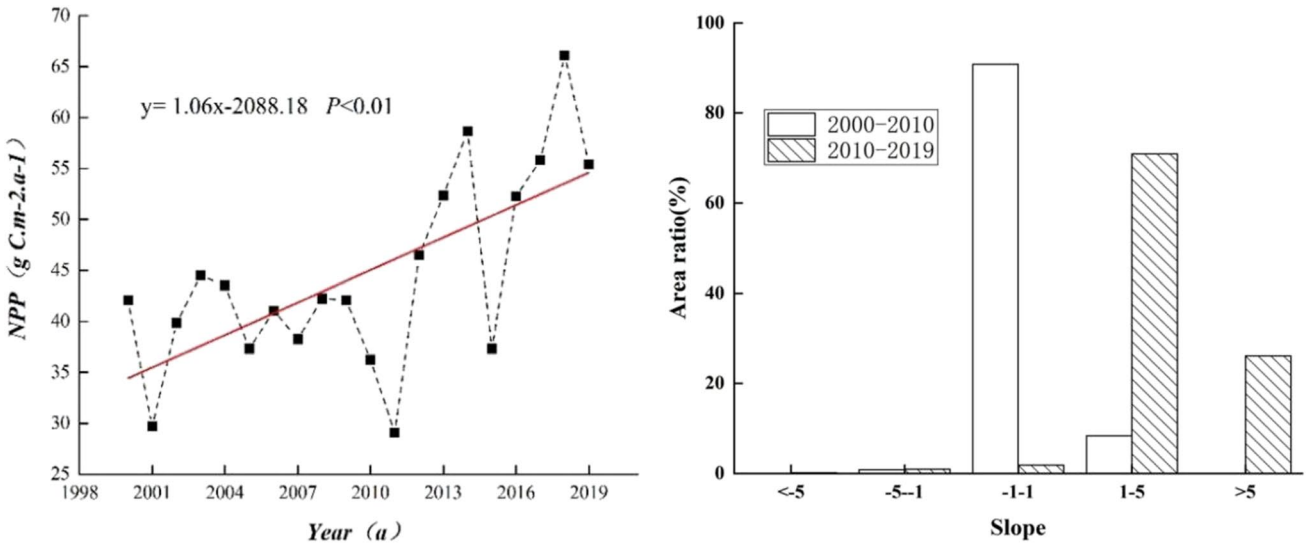

Fig. 4 NPP variation in the study area from 2000 to 2019

a^{-1}, with a multi-annual minimum in 2011 and maximum in 2018 ($P < 0.01$). These values differed by 37.04 g·C ·m^{-2}·a^{-1}.

From 2000 to 2010, the NPP stability ranged from 90.84 to 8.34%, with the highest values occurring in the Dongsheng District of the study area from 2010 to 2019. The mining area showed the greatest interannual variability in an NPP of about 70.91%, followed by 26.13% (Figs. 4 and 5).

As shown in Fig. 6, average annual NPP in the study area generally increased but could be divided into five categories by natural fracture methods. This approach highlights regional average annual NPP values of 40 to 60 g·C·m^{-2}·a^{-1}. These obtain the largest proportion (57.96%) of the study area, followed by the 20 to 40 g·C·m^{-2}·a^{-1} tier, which covers 34.12% of the study area. The NPP range of > 80 g·C·m^{-2}·a^{-1} was obtained in only 0.28% of the study area.

Changes in NPP from 2000 to 2019 exhibit considerable spatial heterogeneity. The area experiencing increased NPP represented 21.54% of the study areas and mainly occurred around Dongsheng, Kangbashi, and Inkinhoro Banner. Areas experiencing decreasing NPP values accounted for 78.46% of the study area (Fig. 7). According to the M-K significance test results (Fig. 8), areas experiencing significant increases in NPP accounted for 1.69%, 1.33%, 18.42%, 0.19%, 0.01%, and 0.12% of the total area. These values generally comported with trends in NPP variation in the study area.

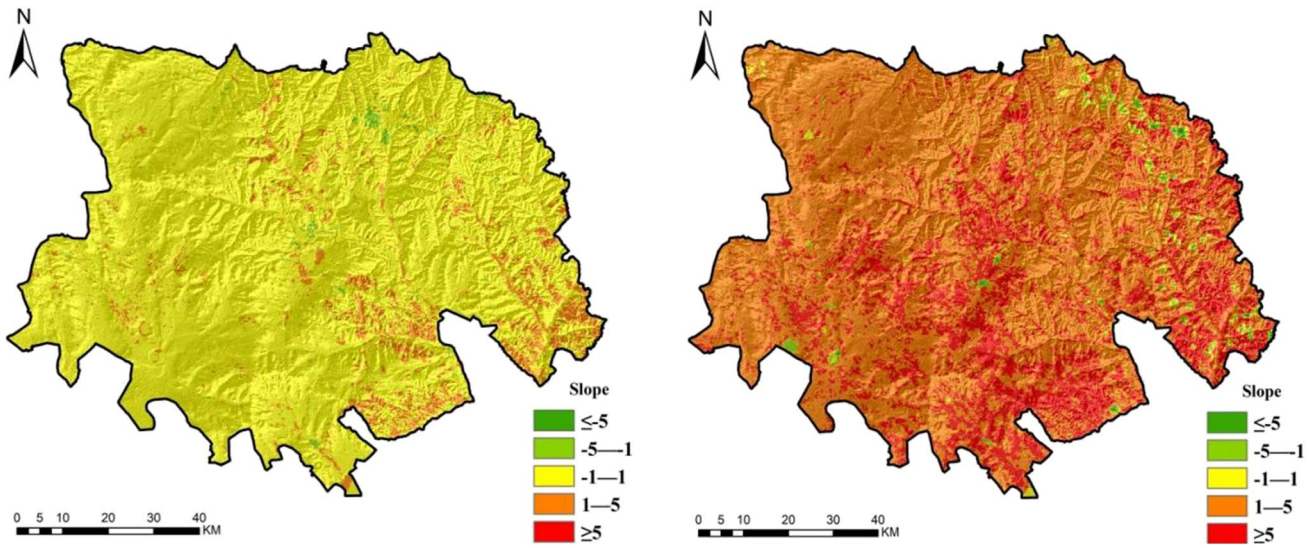

Fig. 5 Spatial distribution of NPP variation in the study area from 2000 to 2010 (left) and 2010 to 2019 (right)

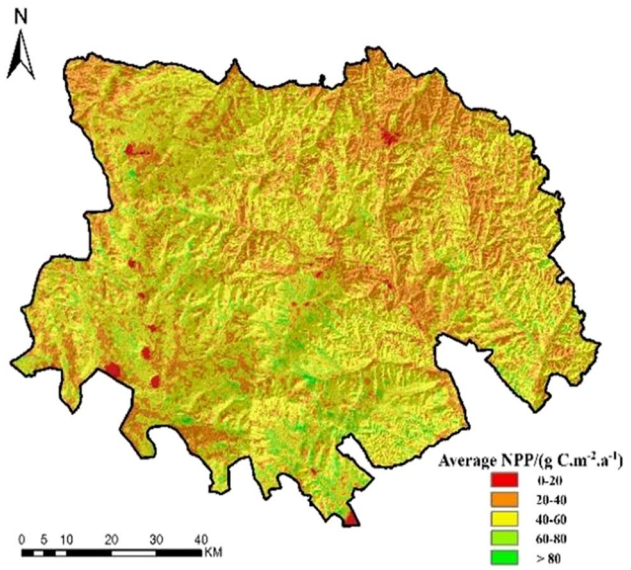

Fig. 6 Spatial distribution of tiered 20-year average NPP values in the study area

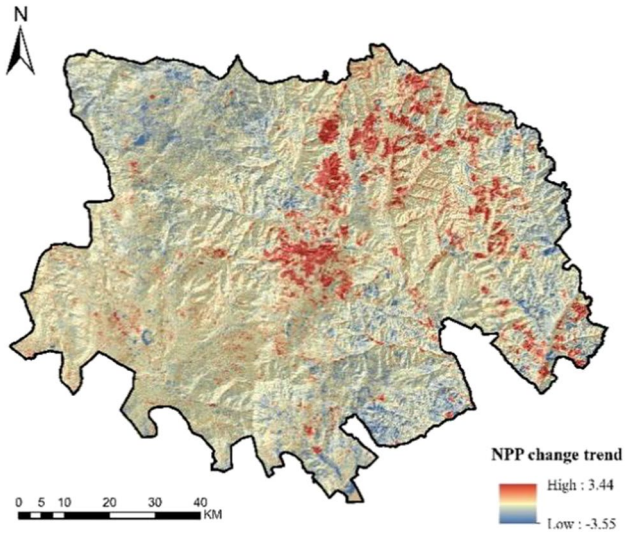

Fig. 7 NPP variation in the study area from 2000 to 2019

The third-phase land-use data indicate the total NPP for the study area in 2000, 2010, and 2019 of 5475.70 kg·C, 4717.96 kg·C, and 7211.90 kg·C, respectively. These demonstrate the overall trend of decline and then increase. Among these values, cultivated land showed the largest contribution to total NPP, accounting for about 59.72% of the total NPP. Grassland made the second largest contribution to total NPP (39.25%) followed by forested land (1%), and other land (0.03%) (Fig. 9).

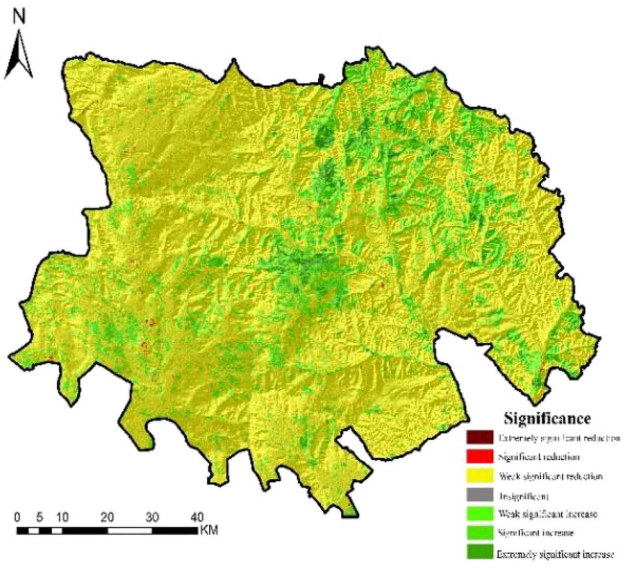

Fig. 8 Significance of interannual variation in NPP in the study area from 2000 to 2019

Changes in landscape type in the study area

The landscape types in the study area primarily consist of cultivated land and grassland, with the former concentrated in the west and south at low altitudes and the latter predominating in the northeast and at higher altitudes (Fig. 10).

From 2000 to 2019, the area of cultivated land declined by about 433.49 km^2, amounting to respective rates of change of − 30.29% and − 0.48%. Forested land expanded by about 12.65 km^2. While this represents a small area, given the general paucity of forested land to begin with, the change amounted to 3.5 and 133 times that observed in the respective base years. Grassland initially expanded and then declined but showed an overall expansion of about 478.33 km^2. This provides a rate of change of 8.4% and 0.9% for the respective base years. The "other" land category showed a slight increase in area and relatively high rates of change of 30.73% and 21.66% for the two base periods. The cultivated land area has continuously declined over the last two decades due to conversion to grassland (342.38 km^2) and land types categorized as "other" (10.04 km^2). The increase in forested land primarily derived from the conversion of cultivated land (5.27 km^2) and meadows (6.73 km^2). The increase in grassland area also derived from the conversion of cultivated land (24.31 km^2) (Table 1).

The landscape pattern index of the study area showed little change from 2000 to 2019. A mean PD of 0.15 indicates increasing fragmentation and smaller patches. The relatively low estimated FRAC values indicate the stable boundaries of land patches. The estimated SPLIT values indicate the

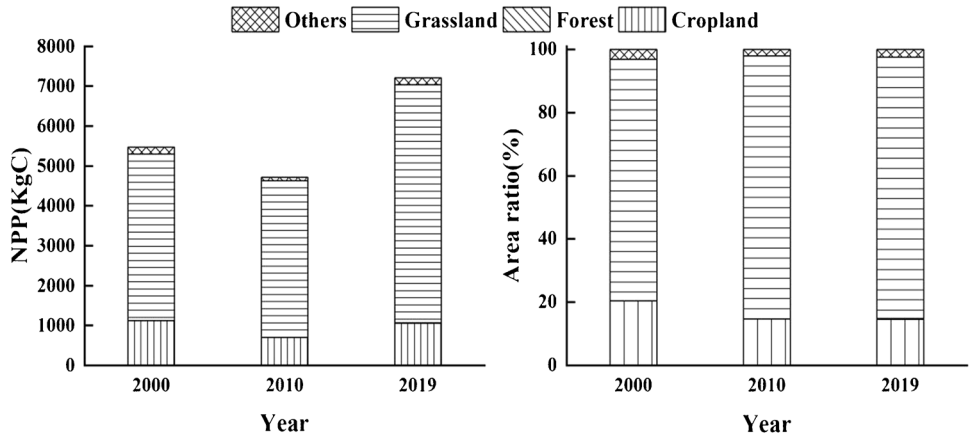

Fig. 9 Total NPP variations in the study area in 2000, 2005, 2010, and 2015

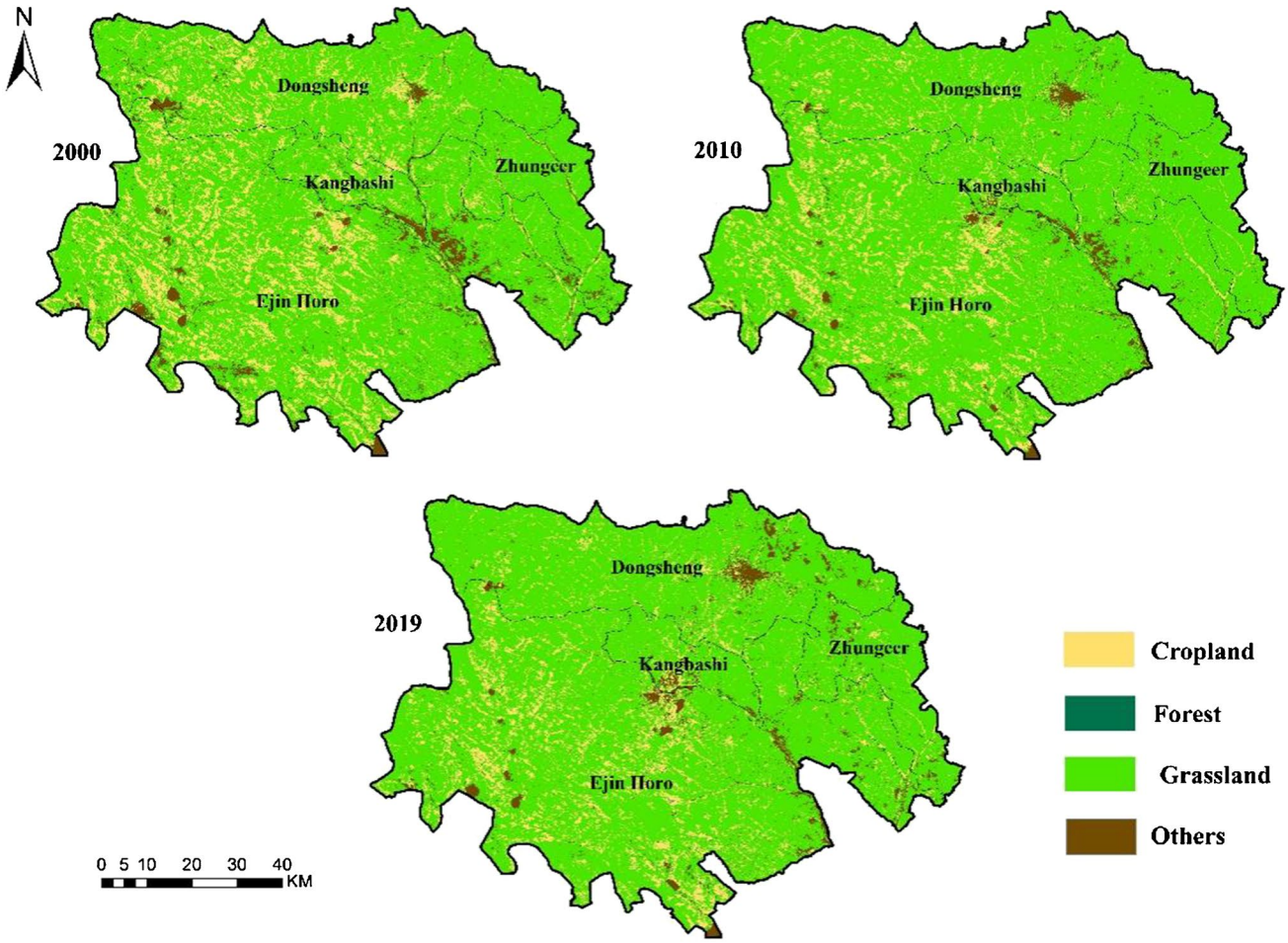

Fig. 10 Land-use changes in 2000, 2010, and 2019

increasing uniformity of different land-use types. Table 2 shows average SHDI years of 1.14, overall increasing plaque type, and an average AI of 75.44. The decrease in AI indicates the less centralized distribution of land types. The five parameters generally indicated increased landscape diversity and less spatial concentration or uniformity in land-use types. The study area shows an increased degree of landscape fragmentation but greater temporal stability of land types.

Table 1 Land-use transfer matrix for the study area from 2000 to 2019 (Ha)*

Initial land type	Grassland	Cropland	Forested	Others
Grassland	593,172.55	73,933.49	0.07	24,313.06
Cropland	34,238.32	62,972.36	0.07	1003.81
Forested	673.05	527.36	1.96	64.85
Others	15,501.44	4130.89		11,169.59

*Given limited area of forested land, values are given in hectares (Ha)

Table 2 Landscape indices for the study area in 2000, 2010, and 2019

Year	PD	FRAC	SPLIT	SHDI	AI
2000	0.17	1.51	3.73	0.73	82.51
2010	0.55	1.53	17.05	1.34	72.06
2019	0.57	1.53	18.17	1.37	71.75

Effects of land-use changes on NPP

Effects of land-use changes on NPP

As shown in Fig. 11, both forested and grassland areas increased between 2000 and 2010. Cultivated land and other land uses decreased. All four land types showed a declining NPP. Between 2010 and 2019, land-use area increased, while the area of cultivated land and grassland decreased. NPP increased in all four land categories.

Table 3 lists the contribution from changes in land-type area to changes in NPP. Changes in land use for each decade promoted NPP by 757.73 kg C and 2493.94 kg C, or showed contribution rates of 44.66% and 93.9% for the respective 2000–2010 and 2010–2019 timeframes.

Correlation between landscape indices and NPP

The landscape index and NPP distribution maps were divided into continuous 1 × 1 km grids, which were then analyzed for correlations between landscape indices and NPP. Invalid and irrelevant values were excluded. From 2000 to 2019, AI showed an inverse correlation with NPP, while all other landscape pattern indices showed positive correlation with NPP (Fig. 12). Principal component analysis of the five landscape pattern index results for three timeframes (2000, 2010, 2019) identified the top ranked components, representing 92.5%, 73.5%, and 60.29% of the variance, respectively. The highest ranked component was significantly positively associated with NPP (significance level of 0.01). The highest ranked principal component for each year was linearly matched to the NPP values (Fig. 13) to show that NPP values in all 3 years increased with the first principal component.

Discussion

Discussion of NPP model results

This research used field, product, and model data to estimate and validate NPP in the study area. Sources of error, such as human errors in field measurements or those arising from imprecision in the finished product data, warranted further analysis and validation of CASA NPP results. The earlier results described by Zhu et al. (2007) for this region served as the basis for comparison. The results described here also generally resembled those published by Mu et al. (2013), who performed an inversion of CASA results from the Inner Mongolia Autonomous Region (Zhu et al. 2005a, b). The results shown here were generally lower than those reported by Xie et al. (2015). The differences in the BLOME-BGC

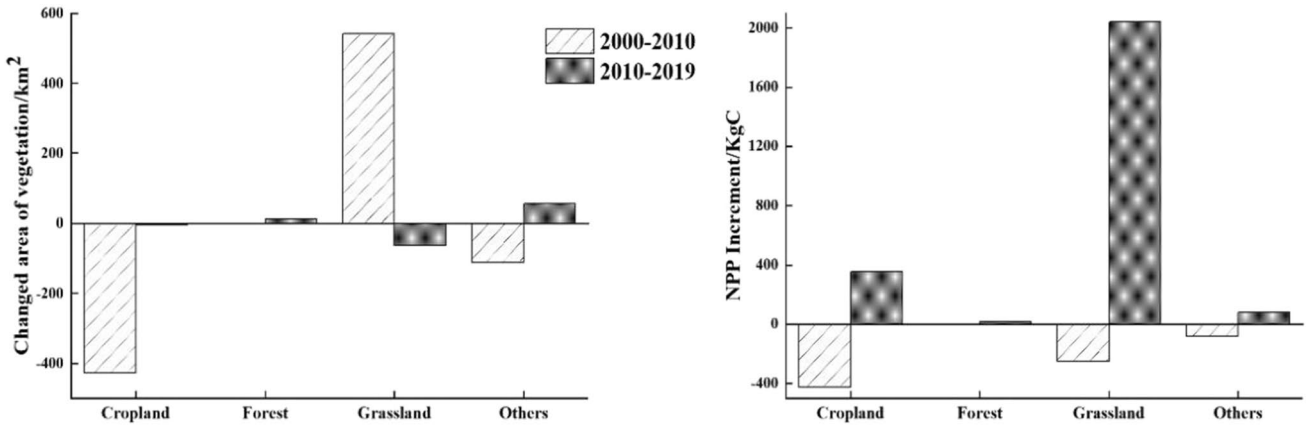

Fig. 11 Changes in NPP of different land-use types

Table 3 Contribution of land-use changes to total NPP variation

Period	Influence by mass (kg C)	Contribution rate (Roc)
2000–2010	757.73	44.66
2010–2019	2493.94	93.9

model results arose from the incompatible time series and spatial scales, as well as differences in the used indices. The basic data interpolation methods and uncertainties in the study area also differed between the two models. Overall, the NPP results obtained in the study area using the model methods resembled field data, finished product data, and previous research data. In accordance with previous research findings, we found a CASA model that was suitable for the vegetation NPP inversion in this study area. However, the estimation of NPP from remote sensing images and other spatial data faces considerable limitations, due to the low spatial and temporal resolution of data and scarce meteorological stations. Given these deficiencies, we limit further interpretations to the present objectives of assessing the impacts of changing land uses in the study area over the last 20 years.

Effects of land-use changes on regional NPP

From 2000 to 2019, total NPP first decreased and then increased, perhaps due to changes in regional land-use types. As a reflection of land-use changes, variations in land type cause different NPP changes in different periods. From 2000 to 2010, total NPP decreased, likely due to the continuous reductions in cultivated land and others land caused by the promotion of the coal mining industry, poor climate conditions, and other factors. The weak growth in forest and grassland during this time indicates the significant impact of forest expansion. Between 2010 and 2019, total NPP increased. During this time, both the grassland and cultivated land areas declined in while forested and other land areas rapidly expanded. The likely influence of urban expansion and the ecological civilization construction policy in the region led to ecological protection, promoted vegetation growth, and increased crop yields among restored areas. Climate conditions also supported higher productivity in this period, and these appear to make the predominant contribution to increase in NPP. The two decades of land-use changes contributed to NPP changes. The continuous growth in total NPP reflects the stronger impact of the NPP growth area compared to that experiencing NPP reductions.

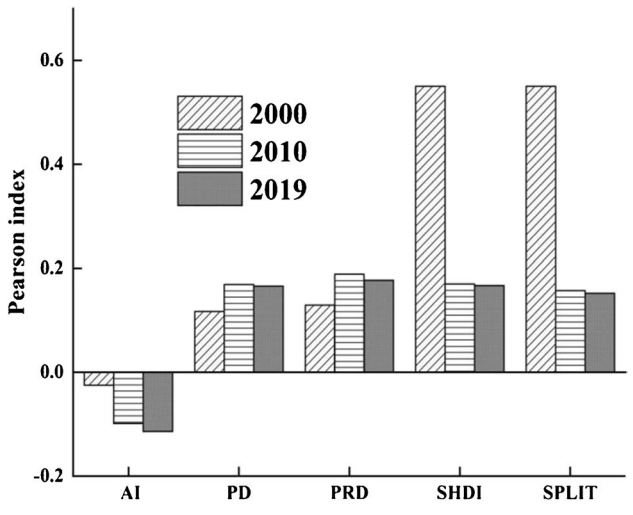

Fig. 12 Correlation between NPP and landscape parameters

Relationship between landscape indices and regional NPP

In addition to AI and other indices, new land-use types influence NPP by reducing more contiguous areas to form smaller, more dispersed patches. The increase in fragmentation increased variations in landscape type and stability. Analysis indicates that the new landscape types can fix more carbon than the original landscape type. However, the loss of a centralized distribution of some landscape types can also reduce total NPP. Principal component analysis of variations in the five landscape indices over 3 years of NPP data found that the increased regional vegetation type, as well as the enhanced cultivation of cultivated land, and forest and grassland land types can improve the regional carbon fixation capacity. The results further indicate that the loss of the original patch type will gradually form stable bodies within the landscape pattern in the mining area. The highest ranked component loading value reached 92.5%. Although the remaining 2 years did not meet the PCA extraction requirements, they exhibited a weak, linear relationship between the landscape pattern index and NPP. The weakness of the relation may relate to the low spatial resolution of the land-use data. Errors associated with landscape indices arise from the variable data accuracy and processing methods, but indices still appear to capture changes in landscape pattern (Kang et al. 2014).

Conclusions

From 2000 to 2019, the overall status of vegetation net primary productivity in Shendong mining area showed a fluctuating upward trend, and changes in these trends had a large spatial heterogeneity. Among them, vegetation NPP showed an increasing trend and was mainly distributed in Dongsheng

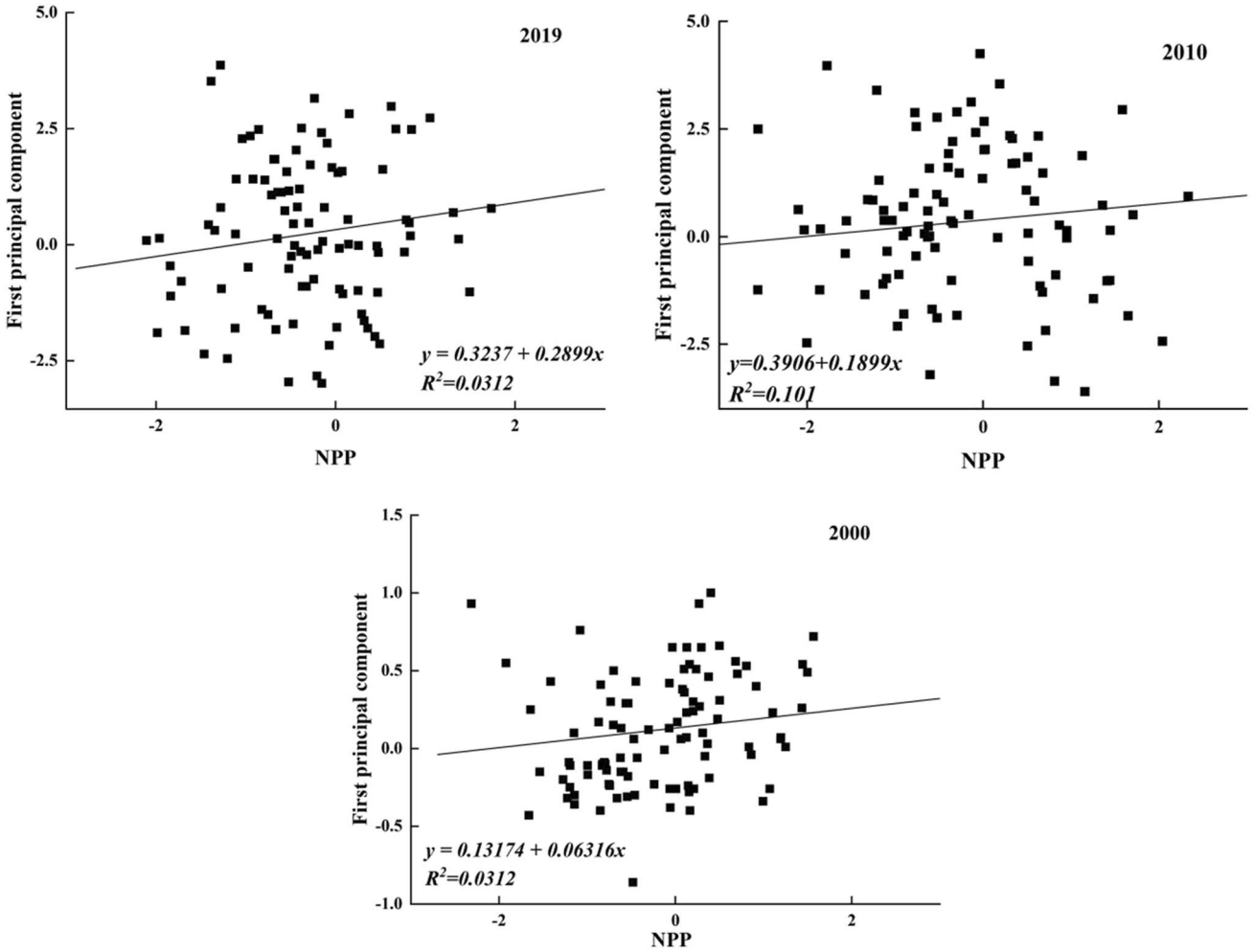

Fig. 13 Relationship between NPP and highest ranked component

District, Kangbashi District, and Ejin Horo Banner. The bordering areas of Ejin Horo Banner and other areas show a decreasing trend. Among them, from 2000 to 2010, the areas with a stable NPP were relatively high, and the remaining areas showed mild growth; from 2010 to 2019, the area of areas with a slight growth in NPP changes accounted for the largest proportion, followed by areas with obvious growth.

From 2000 to 2010, both forest and grassland areas increased, cultivated land and other land uses decreased, and the NPP of the four types of land use decreased. From 2010 to 2019, the area of forest land and other land uses increased, the area of cultivated land and grassland decreased, and the NPP of all four types of land use increased. The land-use changes in the two periods played a role in promoting the growth of NPP, with contribution rates of 44.66% and 93.9%, respectively. In 2000, 2010, and 2019, the total NPP in the study area showed a trend of first decreasing and then increasing. Among these, cultivated land contributed the most to the total NPP, followed by grassland, forest land, and other land.

Among the landscape vegetation indices used during the study period, AI was negatively correlated with NPP; the other four landscape pattern indices were positively correlated with NPP. In 2000, 2010, and 2019, the first principal component was significantly positively correlated with NPP. The NPP in the study area is strongly affected by human activities. In the later period, to maintain the current vegetation status, improving the landscape type and type concentration in the study area can be beneficial to the growth in NPP. The carbon sequestration capacity of vegetation could be improved by optimizing the landscape pattern and through the centralized and contiguous planting of vegetation species in the future.

Numerous studies on ecosystems found that vegetation NPP depends on both natural and human factors (Vahtmäe et al. 2021; Xie et al. 2022). Landscape changes in the study area may reflect local natural conditions and human activities, such as the ecological restoration of mining areas. Climate change influences vegetation growth trends and influences carbon fixation capacity. Coal mining in the study

area led to changes in terrain and hydrological conditions, especially on the surface, which can, in turn, cause changes in landscape types. Ordos is under the construction of ecological civilization environment (sustainable policies) in recent years (Meng et al. 2013). The implemented policies include returning farmland to grass and forest land. Longer-term and previous afforestation also had a further impact on the distribution and growth of local landscape types. In the future, the influence of NPP in the study area can be further studied in combination with other influencing factors.

Author contribution All the authors contributed to the study conception and design. Material preparation, data collection, and analysis were performed by DZ, CH, XC, BL, and LT. The first draft of the manuscript was written by KJ and all authors commented on previous versions of the manuscript. All authors read and approved the final manuscript.

Funding This work was supported by the Technology of Site Quality Improvement in Mining Subsidence Area (Grant number ZDZX2018058). Author Ke Jia received research support from School of Geography Science, Inner Mongolia Normal University.

Data availability Not applicable.

Declarations

Ethical approval This section is not applicable to this manuscript.

Consent to participate All the authors have given informed consent to the manuscript.

Consent to publish All the authors have approved the manuscript and agree with its submission to the Environmental Science and Pollution Research.

Competing interests The authors declare no competing interests.

References

Fyllas NM, Bentley LP, Shenkin A, Asner GP, Atkin OK, Diaz S (2017) Solar radiation and functional traits explain the decline of forest primary productivity along a tropical elevation gradient. Ecol Lett 20(6):730–740. https://doi.org/10.1111/ele.12771

Ge W, Deng L, Wang F, Han J (2021) Quantifying the contributions of human activities and climate change to vegetation net primary productivity dynamics in China from 2001 to 2016. Sci Total Environ 773:145648–145648. https://doi.org/10.1016/J.SCITOTENV.2021.145648

Guang X, Bao ZC (2019) Generating a series of land covers by assimilating the existing land cover maps. ISPRS J Photogramm Remote Sens 147:206–214. https://doi.org/10.1016/j.isprsjprs.2018.11.018

Hou MJ, Gao JL, Ge J, Li YC, Liu J, Yin JP, Feng QS, Liang TG (2020) An analysis of dynamic changes and their driving factors in marsh wetlands in the eastern Qinghai-Tibet Plateau. Acta Prataculturae Sinica 29(01):13–27. CNKI:SUN:CYXB.0.2020–01–003

Hu TH, Chang J, Liu XX, Feng SS (2018) Integrated methods for determining restoration priorities of coal mining subsidence areas based on green infrastructure: a case study in the Xuzhou urban area, of China. Ecol Indic 94:164–174. https://doi.org/10.1016/j.ecolind.2017.11.006

Kang SRL, Niu JM, Zhang Q, Han YJ, Dong JJ, Zhang J (2014) Impacts of mining on landscape pattern and primary productivity in the grassland of Inner Mongolia: a case study of Heidaigou open pit coal mining. Acta Ecol Sin 11:2855–2867. https://doi.org/10.5846/stxb201304040603

Li CY, Cui XM, Guo ZZ, Yuan DB, Hu QF (2009) Distribution of mining fissures induced fully mechanized caving mining and analysis on their evolvement characteristics. Min Saf Environ Protect. 36(04):65–68+91. https://doi.org/10.3969/j.issn.1008-4495.2009.04.023

Li W, Chen LQ, Zhou TJ, Zhang K, Li L (2011) Research progress of soil quality in China mining subsidence area. Coal Sci Technol 39(05):125–128

Liu K, Yang YY, Shi RG, (2021) Spatiotemporal changes in forces driving landscape patterns in the Yuqiao Reservoir Watershed during 1990–2021. J Agric Resour Environ 1–15. https://doi.org/10.13254/j.jare.2021.0760

Meng JJ, Aimu RL, Liu Y, Xiang YY (2013) Study on relationship between livelihood capital and livelihood strategy of farming and grazing households: a case of Uxin Banner in Ordo. Acta Scientiarum Naturalium Universitatis Pekinensis 02:321–328. https://doi.org/10.13209/j.0479-8023.2013.046

Mu SJ, Li JL, Zhou W, Yang HF, Zhang CB, Ju WM (2013) Spatial-temporal distribution of net primary productivity and its relationship with climate factors in Inner Mongolia from 2001 to 2010. Acta Ecol Sin 12:3752–3764. https://doi.org/10.5846/stxb201205030638

Potter CS, Randerson JT, Field CB, Matson PA, Vitousek PM, Mooney HA (1993) Terrestrial ecosystem production: a process model based on global satellite and surface data. Global Biogeochem Cycles 7(4):811–841. https://doi.org/10.1029/93GB02725

Vadrevu KP, Justice C, Prasad T, Prasad N, Gutman G (2015) Land cover/land use change and impacts on environment in South Asia. J Environ Manage 148:1–3. https://doi.org/10.1016/j.jenvman.2015.07.054

Vahtmäe E, Kotta J, Argus L, Kotta M, Kotta I, Kutser T (2021) A model-based assessment of canopy-scale primary productivity for the Baltic Sea benthic vegetation using environmental variables and spectral indices. Remote Sens 14(1). https://doi.org/10.3390/rs14010158

Wang H, Li X, Long H, Gai Y, Wei D (2009) Monitoring the effects of land use and cover changes on net primary production: a case study in China's Yongding River basin Elsevier. For Ecol Manage 2009(12):2654–2665. https://doi.org/10.1016/j.foreco.2009.09.028

Xiao T, Wang J, Chen Z (2010) Vulnerability of grassland ecosystems in the Sanjiangyuan region based on NPP. Resour Sci 32:323–330. Google Scholar. CNKI:SUN:ZRZY.0.2010-02-022

Xie SS, Ma C, Tian SJ, Tian JG (2015) NPP changes and climate impact of Shendong coalfield from 2000 to 2010. J Geomatics Sci Technol 01:47–51. https://doi.org/10.3969/j.issn.1673-6338.2015.01.010

Xie JL, Lu ZX, Feng K (2022) Effects of climate change and human activities on aeolian desertification reversal in Mu Us Sandy Land, China. Sustainability 14(3). https://doi.org/10.3390/su14031669

Xu ZJ, Zhang Y, Yang JS, Liu FW, Bi RT, Zhu HF, Lv CJ, Yu J (2019) Effect of underground coal mining on the regional soil organic carbon pool in farmland in a mining subsidence area. Sustainability 11(18). https://doi.org/10.3390/su11184961

Yu MC (2013) Ecological civilization is the road for constructing socialism with Chinese characteristics—thinking of highly promoting the strategy of construction of ecological civilization in the 18th National Congress of CPC. Guihai Tribune 29(01):20–28

Zhang RP, Guo J, Zhang YL (2020) Spatial distribution pattern of NPP of Xinjiang grassland and its response to climatic changes. Acta Ecol Sin 40(15):5318–5326. https://doi.org/10.5846/stxb201901270204

Zhang ZQ, Liu H, Zuo QT, Yu JT, Li Y (2021) Spatiotemporal change of fractional vegetation cover in the Yellow River Basin during 2000–2019. Resour Sci 04:849–858. https://doi.org/10.18402/resci.2021.04.18

Zhao MS, Heinsch FA, Nemani RR, Running SW (2005) Improvements of the MODIS terrestrial gross and net primary production global data set. Remote Sens Environ 95(2):164–176. https://doi.org/10.1016/j.rse.2004.12.011

Zhu WQ, Pan YZ, Long ZH, Chen YH, Li J, Hu HB (2005) Estimating net primary productivity of terrestrial vegetation based on GIS and RS: a case study in Inner Mongolia, China. J Remote Sens 03:300–307. https://doi.org/10.3321/j.issn:1007-4619.2005.03.012

Zhu WQ, Chen YH, Xu D, Li J (2005) Advances in terrestrial net primary productivity estimation models. Chin J Ecol 03:296–300. https://doi.org/10.3321/j.issn:1000-4890.2005.03.014

Zhu WQ, Pan YZ, Zhang JS (2007) Estimation of net primary productivity of Chinese terrestrial vegetation based on remote sensing. Chinese J Plant Ecol 03:413–424. https://doi.org/10.17521/cjpe.2007.0050

Zhuang CW, OY ZY, Xu WH, Zheng H, Wang XK, Bai Y (2009) Spatial pattern of ecosystems in Haihe River Basin based on MODIS data. Chinese J Ecol 06:1149–1154. http://159.226.240.226/handle/311016/5304